SUPPLEMENTAL MATERIALS

Supplemental methods

Sequence alignment

Alignment of yUtp24 and hUTP24 amino acid sequences was performed using ClustalX v. 2.0.11 (http://www.clustal.org) and visualized with JalView (http://www.jalview.org).

Microbial strains and construction of plasmids

Bacterial and yeast strains used in this study are listed in Supplemental Table S1 and the primers in Supplemental Table S2. Plasmids used or constructed in this work are listed in Supplemental Table S3.

ADZY799 *S. cerevisiae* strain (encoding fusion of yUtp24 WT with protein A tag-TEV protease cleavage site and TRP selection marker) was created by homologous recombination. A wild-type diploid BMA64 strain was transformed with DNA fragment containing 5' and 3' overhangs allowing its insertion into the *UTP24* gene upstream its STOP codon. The fragment was obtained in PCR with ADZKD170-ADZKD171 primer pair and using pBS1479 plasmid as template, thus introducing a tag and a selection marker downstream *UTP24* ORF. The production of yUtp24 with protein A tag was validated by western blot analysis using peroxidase-anti-peroxidase (P-A-P) antibodies. The correctness of the *yUTP24* ORF sequence was confirmed by sequencing of the PCR product obtained with use of ADZKD172 and ADZKD173 primers on genomic DNA samples isolated from selected transformants as templates.

To generate ADZY800, a wild-type diploid BMA64 strain was transformed with integration cassette encompassing a fragment of *yUTP24* ORF (with putative catalytic mutation corresponding to D138N substitution) and tag and selection marker sequences. The cassette to be incorporated into *UTP24* locus by *in vivo* recombination was amplified in a three-step PCR as follows. First, a 5' fragment of the cassette with part of *yUTP24* ORF covering sequence with mutation of interest was amplified using ADZKD174-ADZKD175 primer pair and pU24-7 plasmid (see below) as a template. 3' fragment of the cassette (containing TEV site-protein A tag and TRP selection marker sequence with 3' overhang for homologous recombination into *UTP24* locus upstream the termination codon) was amplified using ADZKD176-ADZKD171 primer pair and genomic DNA isolated from ADZY799 strain as template. The full-length amplicon with desired mutation was obtained

with ADZKD174-ADZKD171 primer pair in overlap PCR (where products of the initial 5' and 3' amplifications served as templates), and was subsequently used for transformation. Validation of the obtained strain was performed as in the case of ADZY799.

Plasmids pU24-1 and pU24-2 were generated by inserting *yUTP24* and *hUTP24* open-reading frames amplified from cDNA synthesized by oligo(dT)-primed reverse-transcription on total RNA isolated from yeast and human cells, using primer pairs yU24slicF-yU24slicR and hU24slicF-hU24slicR, respectively, into *Bam*HI and *Xho*I sites of the pET28M-6xHis-SUMOTag vector. The sequence and ligation independent cloning (SLIC) technique was employed. Plasmids pU24-3 and pU24-4 were generated by site-directed mutagenesis with oligonucleotide pairs yU24mutF-yU24mutR or hU24mutF-hU24mutR, using pU24-1 or pU24-2 as templates, respectively. The inserts were sequenced using SumoF primer (**Table S2**).

Plasmids pU24-5 and pU24-6 were obtained by standard cloning of *yUTP24* ORF amplified using primer pairs yU24cmpL-yU24cmpR or yU24cmpL-yU24flcmpR, respectively, and pU24-1 as template into the *Xba*I and *Sal*I sites of the p415 vector. Plasmids pU24-7 and pU24-8 were created similarly, but utilizing pU24-3 as template. Plasmids pU24-9 and pU24-10 were generated by cloning *hUTP24* ORF amplified using primer pairs hU24cmpL-hU24cmpR or hU24cmpL-hU24flcmpR, respectively, and pU24-2 as template into the *Xba*I and *Sal*I sites of the p415 vector. Plasmids pU24-11 and pU24-12 were constructed similarly, but utilizing pU24-4 as template. The inserts were sequenced using p415-left primer (**Table S2**).

Plasmids pU24-13, pU24-14 and pU24-15 were generated by amplifying various fragments of yeast rDNA unit on total genomic DNA isolated from *S. cerevisiae* BY4741 strain as a template with primer pairs pEXseq1-pExseq2, pEXseq3-yITS2b or pEXseq4-pEXseq5, respectively, and cloning them into pCR™-Blunt II-Topo® vector, according to Zero Blunt® TOPO® PCR Cloning Kit (Invitrogen) manual. Plasmid pU24-16, bearing a fragment of human rDNA unit was obtained in the same way, but using 3637For-3971Rev primer pair and total genomic DNA isolated from human HeLa cells as template.

Plasmid pcDNA5/FRT/TO(2xTEV) – a derivative of pcDNA5/FRT/TO with two TEV cleavage sites was constructed as follows. pcDNA5/FRT/TO was linearized with *Bam*HI and *Eco*RV restriction enzymes and served as a template for amplification with primer pair 0I.For-0I.Rev. Obtained PCR product was used as a

template in second round of amplification, employing 0II.For-0II.Rev primer pair. Resulting amplicon was then circularized via SLIC.

Plasmid pcDNA5/FRT/TO(2xTEV)-C-FLAG was obtained by SLIC-mediated circularization of the PCR product generated with p3.For-p3.Rev primer pair using pcDNA5/FRT/TO(2xTEV) pre-linearized with *Eco*RV and *Xho*I, as template. Plasmid pcDNA5/FRT/TO(2xTEV)-N-eGFP was generated by inserting eGFP ORF amplified using p2.For-p2.Rev primer pair with pEGFP-C1 as template, via SLIC into pcDNA5/FRT/TO(2xTEV) digested with *Afl*II and *Bam*HI. Plasmid pcDNA5/FRT/TO(2xTEV)-C-eGFP was constructed likewise, but employing p4.For-p4.Rev primer pair and pcDNA5/FRT/TO(2xTEV) linearized with *Eco*RV and *Xho*I, as an acceptor.

Plasmids pU24-17 and pU24-18 were constructed by inserting hUTP24 amplified using hU24pcd5F-hU24pcd5R primer pair with pU24-2 or pU24-4 as template, respectively, via SLIC into pcDNA5/FRT/TO(2xTEV)-C-FLAG digested with *Age*I and *Nhe*I. The inserts were sequenced using FRTT_F and FRTT_R primers. Plasmid pU24-19 was created by inserting the PCR product obtained as for pU24-17 via SLIC into pcDNA5/FRT/TO(2xTEV)-N-eGFP linearized with the same enzymes. The insert was sequenced using EGFP_F and FRTT_R primers. Plasmids pU24-20 and pU24-21 were generated similarly to pU24-17 and pU24-18, but pcDNA5/FRT/TO(2xTEV)-C-eGFP was used as an acceptor. The inserts were sequenced using FRTT_F and EGFP_R primers.

A multistep cloning procedure for generation of vectors for co-expression of recoded hUTP24 with FLAG epitope at the C-terminus [wild type (WT) variant or its catalytic mutant counterpart (mut)] and sh-miRNAs directed against endogenous hUTP24 mRNA was the following.

First, we performed a search for 3 miRNA sequences that should specifically and efficiently target endogenous hUTP24 mRNA, using BLOCK-iT™ RNAi Designer tool from Invitrogen (with "*miR RNAi"* option) (http://rnaidesigner.invitrogen.com/rnaiexpress). We chose candidate sequences starting at positions 475, 501 and 552 of hUTP24 ORF. Basing on the general idea of BLOCK-iT™ Pol II miR RNAi Expression Vector Kits from Invitrogen (http://www.invitrogen.com/site/us/en/home/Products-and-Services/Applications/rnai/Vector-based-RNAi/Pol-II-miR-RNAi-Vectors.html), we then designed a synthetic DNA fragment, encompassing combination of miRNA sequences listed above. It encoded three tandemly

positioned shRNAs corresponding to pre-designed miRNAs – so-called sh-miRs, where sense and antisense miRNA sequences were separated by the loop element enabling formation of the hairpin (**Fig. S13**). Each of the sh-miR sequences was flanked at both termini with motifs ensuring correct miRNA processing from the artificial pre-miRNA precursor, following a natural miRNA biogenesis pathway active in human cells (**Fig. S13**). In addition, polyadenylation signal derived from the gene encoding herpes simplex virus thymidylate kinase (HSV-TK-PA) was placed at the 3'-end of this synthetic cassette, allowing for correct termination of transcription in human cells (**Fig. S13**). The cassette contained *Eco*RI/*Sal*I and *Bsu*15I/*Hin*dIII restriction site combinations at the 5' and 3' extremities, respectively, which were used in subsequent cloning steps (**Fig. S13**). It was synthesized by BlueHeronBio company (http://blueheronbio.com) and inserted between *Eco*RI and *Hin*dIII sites of pUCAmpMinusMCS vector (**Fig. S14**). Next, a sequence encoding eGFP (allowing for monitoring of expression of the cassette containing artificial pre-miRNA) was amplified in PCR using eGFPFor-eGFPRev primer pair and pEGFP-N1 plasmid (Clontech) as a template and inserted into *Eco*RI and *Sal*I sites of the provided [pUCAmpMinusMCS] *tri-miR* plasmid, thus giving [pUCAmpMinusMCS] *eGFP-tri-miR* transitory construct (**Fig. S14**, *step A*). Additionally, a site recognized by *Xma*JI restriction endonuclease was introduced in eGFPFor oligonucleotide upstream the 5'-end of eGFP ORF (**Fig. S14**), which was used at further cloning stage. The insert was sequenced using pUCmMCSF and pUCmMCSR primers (**Table S2**).

In the next phase of construct generation, it was necessary to modify the sequence of exogenous hUTP24 ORF in order to make it insensitive to miRNA action. To this end, we ordered synthesis of recoded hUTP24 open reading frame (see **Fig. S15** for nucleotide sequence alignment of original and recoded hUTP24 ORF fragment). The idea of recoding was to introduce synonymous mutations into all possible codons (at those positions where degeneration of genetic code could be utilized and taking codon usage frequency into account), particularly within the fragment containing sites recognized by miRNA, so that the sequence would be as much divergent from the initial one as possible (**Fig. S15**). We ordered WT and mut variants of recoded ORF, introducing additionally: restriction site (*Mlu*I) and Kozak sequence at the 5'-end; and sequence coding for FLAG-tag, encompassing STOP codon and restriction site (*Apa*I) at 3' end; both variants were provided by BlueHeronBio as inserts cloned into pUCAmpMinusMCS. Subsequently, they were transferred into *Mlu*I and *Apa*I sites of BI-16 vector, thus replacing hRLUC ORF present therein, with the use of *E. coli* MH1 strain (**Fig.**

S14, *step B*). This way, [BI-16'] *hUTP24rec WT* and [BI-16'] *hUTP24rec mut* transitory vectors were constructed. The presence of recoded fragment was checked by digestion with *Nco*I restriction enzyme and sequencing using primers BIseq_F and BIseq_R (**Table S2**).

The aim of the ultimate cloning stage was to transfer a DNA fragment containing a co-cistron of eGFP coding sequence and pre-miRNA/HSV-TK-PA from [pUCAmpMinusMCS] *eGFP-tri-miR* construct to the BI-16 vector derivative from the previous step, through replacement of the FLUC ORF present in the latter. To this end, all plasmids were propagated in *E. coli* dam-/dcm- strain prior to the standard cloning procedure, utilizing *Xma*JI and *Bsu15*I restriction sites (**Fig. S14**, *step C*), followed by transformation of the ligation products into *E. coli* MH1 strain. This eventually led to the generation of final constructs: pU24-22 and pU24-23 (**Table S3**). Both *hUTP24* and *eGFP-tri-miR* inserts were sequenced using primers BIseq_F, BIseq_R, UTP_R330, BI16seq1 and BI16seq2 (**Table S2**).

Yeast complementation assays

The *S. cerevisiae yUTP24 tet::off* strain (see **Table S1**) was transformed with p415 vector derivatives bearing different versions of yUtp24 and hUTP24 (pU24-5 – pU24-12). The empty p415 vector served as a negative control. Transformants were selected on plates with synthetic complete medium without leucine (SC-leu), containing ampicillin and G418.

In the streaking test, approximately equivalent amounts of inoculum from each transformed strain were streaked onto SC-leu+amp+G418 (allowing for expression of endogenous *yUTP24*) and SC-leu+amp+G418 plates containing 20 µg/ml doxycycline (repressing chromosomal *yUTP24* expression). In the droplet assay, transformants were cultivated in SC-leu+amp+G418 liquid medium at 30°C overnight and then serial dilutions (10^0-10^{-4}) of cultures having approximately the same OD_{600} (≈0.3) were spotted onto two SC-leu+amp+G418 plates in the absence or presence of doxycycline (20 µg/ml). Cell growth was analyzed after 48 h of incubation at 30°C.

Yeast cultures

The *S. cerevisiae yUTP24 tet::off* strain derivatives transformed with p415 empty vector, pU24-5 plasmid or pU24-7 construct were grown in 25 ml of SC-leu+amp liquid medium overnight at 30°C. The next day, pre-cultures were diluted in 200 ml of either fresh SC-leu+amp to OD_{600}≈0.005 or SC-leu+amp+dox to OD_{600}≈0.005

(in the case of pU24-5 transformed strain) or to OD_{600}≈0.1 (for p415 and pU24-7 transformed strains, growing much slower when endogenous yUtp24 was depleted). After 14 hours of incubation with shaking at 30°C, OD_{600} value for all cultures amounted to approximately 0.5.

Immunofluorescence and microscopy analysis

$1.5x10^5$ HeLa cells were grown on coverslips placed in 6-well plates for 12 hours and transfected transiently with 1 µg of pU24-16 construct using 1.5 µl of TransIT-2020 Transfection Reagent (MirusBio) according to the manufacturer's recommendations. 2 hours following transfection medium was replaced with a fresh one. In case of Hek293 Flp-In T-REx-derived stable cell lines, $2x10^4$ cells were plated onto Nunc Lab-Tek II 8-well chamber slides (Thermo Scientific), pre-coated with Poly-D-Lysine (Sigma-Aldrich), in a medium with doxycycline (100 ng/ml) to induce protein expression.

Following aspiration of the medium, cells were fixed with 3.7% formaldehyde/5% sucrose in PBS for 25 min, permeabilized with 0.5% Triton X-100/10% FBS solution in PBS for 15 min and blocked for 30 min with 10% FBS solution in PBS (blocking solution). Cells were incubated in blocking solution, first with primary antibody for 1 h and then with secondary antibody coupled to fluorophore for 1 h in the dark. Finally, cells were stained with DAPI (Invitrogen) by incubation in a 2.5 µg/ml solution in PBS for 5 min and washed as above. All procedures were performed at 25°C and cells were washed 3 times with PBS between each step. After the final wash coverslips were mounted on chamber slides in ProLong Gold antifade reagent (Invitrogen), left in the dark overnight at 25°C and then stored at 4°C until microscopic analysis.

The following antibodies were used (dilutions in parentheses): 1) primary – mouse monoclonal anti-FLAG (M2) (Sigma-Aldrich; F3165) (1:200); rabbit polyclonal anti-fibrillarin (Abcam; ab5821) (1:150); 2) secondary – Alexa Fluor 488-conjugated donkey anti-mouse, Alexa Fluor 555-conjugated goat anti-rabbit IgG (both from Molecular Probes) (1:800). Imaging was performed on a FluoView FV1000 system with spectral detectors (Olympus), using appropriate emission filters and a 60x/1.40 oil immersion objective lens. Images were processed using the FluoView software.

FACS analysis of eGFP expression

Stable inducible human HeLa Flp-In T-REx-derived cell lines were plated at the density of $3×10^5$ cells per well in 6-well plate, and cultured for 24 h in a medium containing doxycycline or without the inducer. After that

time cells were detached from the plate by scraping in PBS. Then, the cells were centrifuged at 500xg for 3 minutes, washed with PBS, centrifuged again and resuspended in 0.5 ml of PBS. Fluorescence was measured using a FACScalibur instrument (BD Biosciences). Data was analyzed using Cyflogic software (CyFlo Ltd.).

Metabolic activity assay

Cells (5×10^3 or 2×10^3) of the stable inducible human HeLa Flp-In T-REx-derived cell lines were plated in triplicate (for each cell line and condition) in 96-well plates (100 µl total volume in each well). Cells were either cultured in a medium lacking doxycycline or subjected to treatment with the inducer. 72 h after induction 10 µl of AlamarBlue® (Invitrogen) was added directly to each well and the plates were then incubated at 37°C to allow the cells to convert resazurin to resorufin. Fluorescence signal was measured after 240 min using the DTX880 Multimode Detector (Beckman Coulter).

Western blotting

Protein samples from yeast cultures and human cell lines were prepared according to standard protocols, resolved in 10-12% SDS-PAGE gels, and immobilized on Protran nitrocellulose membranes (Whatman) by electrotransfer using Trans-Blot® SD Semi-Dry Transfer Cell (Bio-Rad). Following transfer, membranes were stained with Ponceau S Red (Sigma-Aldrich; 0.1% in 3% acetic acid), blocked in 5% non-fat milk in TBS containing 0.05% Tween-20 (TBST), and incubated in the same solution with primary antibodies. The following primary antibodies were used for analyses: rabbit polyclonal anti-FLAG (Sigma-Aldrich; F-7425), rabbit polyclonal anti-hUTP24 (anti-FCF1) (Abcam; ab95301), mouse monoclonal anti-eGFP (B2) (Santa Cruz Biotechnology; sc-9996), mouse monoclonal anti-hXRN2 (H-3) (Santa Cruz Biotechnology; sc-365258), rabbit polyclonal anti-NOL12 (Bethyl Laboratories, Inc; A302-732A) and rabbit polyclonal anti-DXO1/DOM3Z (Proteintech; 11015-2-AP). Membranes were then washed with TBST and incubated with appropriate secondary antibody [goat anti-rabbit, goat anti-mouse (Calbiochem; 401393, 401215, respectively) conjugated with horseradish peroxidase. Blots were developed in a Curix 60 machine (AGFA) using the Immun-Star™ WesternC™ Kit (Bio-Rad) and CL-XPosure™ Films (Thermo Scientific).

Reverse transcription and quantitative PCR

Total RNA for qPCR was isolated from stable HeLa Flp-In T-REx human cell lines grown in the absence or in the presence of doxycycline. 10 µg of total RNA was treated with 4 units of TURBO™ DNase (Ambion) in the

presence of RiboLock™ RNase Inhibitor (Thermo Scientific), according to the guidelines of the manufacturer. Following phenol:chloroform extraction and precipitation of RNA with isopropanol, 2 µg of DNase-treated RNA was used for cDNA synthesis. To analyze levels of the mature hUTP24 mRNA, reverse transcription was performed using a mixture of 50 pmol of an oligo(dT) primer, 250 ng of random hexamers (Invitrogen) and Superscript III™ reverse transcriptase (Invitrogen), according to the manufacturer's instructions, in a final volume of 20 µl. For the analysis of CamKI mature mRNA levels, RNA was reverse transcribed as above, but using only oligo(dT) primer. For detection of CamKI pre-mRNA containing first (In1J) or second (In2J) intron, reverse transcription was performed using a mixture of appropriate CamKI pre-mRNA gene-specific primer (CamKI In1J_RT rev or CamKI In2J_RT rev, respectively) and a primer specific to GAPDH (GAPDH_RT rev) (2 pmol each). cDNA samples were diluted 10-fold and mixed with Platinum® Quantitative PCR SuperMix-UDG (Invitrogen), 2.5 pmol of each oligonucleotide (**Table S2**) and 0.5 µg of bovine serum albumin in a final volume of 10 µl. Real-time PCR was carried out in a Roche LightCycler® 480 system. Negative controls lacking reverse transcriptase were included for each experiment and showed a negligible background. The specificity of the reaction was verified by melt curve analysis. Analyses were performed in triplicate. GAPDH mRNA was amplified as an internal control and used for normalization.

siRNA transfection

For *hXRN2* gene silencing, the model stable inducible cell lines derived from HeLa Flp-In T-REx cells were grown to 30-40% confluence, either in the absence or in the presence of doxycycline, and subjected to Stealth siRNA (Invitrogen) transfection. Transfections were performed in Ø100 mm culture dishes using Lipofectamine RNAiMAX (Invitrogen) according to the manufacturer's recommendations. The Stealth siRNA specific for *hXRN2*, *NOL12* and *DXO1/DOM3Z* silencing, with oligo IDs: HSS176944, HSS149137 and HSS102885, respectively, as well as a negative control (Stealth RNAi™ Negative Control LO GC) were used at the final concentration of 20 nM.

Supplemental Discussion

U3 snoRNA-dependent processing at site A_1, the role of the UTP24 protein in this event in yeast and humans, and the outcome of abolishing catalytic activity of this factor may also largely depend on the interactions between U3 snoRNA and pre-rRNA. While interactions between U3 snoRNA and the 18S rRNA segment are ubiquitously conserved, those involving sequences within 5'-ETS vary substantially between different species, as delineated below.

U3 snoRNA in different organisms forms a structure that can be subdivided into three functional parts: 1) 5'-domain, encompassing highly evolutionary-conserved GAC element and boxes A and A'. This conservation is associated with high similarity in the 18S rRNA regions complementary to this U3 snoRNA domain in various species (**Fig. S12A-D**);[1] 2) the variable hinge region, the sequence of which apparently co-evolved with the sequences of 5'-ETS to enable interactions between U3 snoRNA and pre-rRNA in a given organism. Interestingly, while sequences of the hinge region differ significantly between species, location of the elements base-pairing with 5'-ETS sites with regard to the 5'-end of U3 snoRNA is comparable (**Fig. S12A-D**); and 3) the 3'-domain, which is required for nucleolar localization of U3 snoRNA and serves as a scaffold for binding U3 snoRNA-associated proteins, thus forming a U3 snoRNP subcomplex of the SSU processome.[1, 2] U3 snoRNA regions involved in its docking on the pre-rRNA are the 5'-domain and the hinge region (**Fig. S12A-D**).[3] The box A base-pairs with the 18S rRNA segment downstream of the A_1 processing site (**Fig. S12A-D**).[3] Formation of the U3 snoRNA box A-pre-rRNA duplex engages the same bases in 18S rRNA, which in its mature form are involved in a conserved long-range tertiary intramolecular interaction, called a central pseudoknot (marked with asterisks in **Fig. S12A-D**).[2, 3] An important role of the U3 snoRNA-pre-rRNA interactions is therefore to prevent formation of the pseudoknot until the correct stage in the ribosome assembly process ocurs, which is when the 18S rRNA is released from the precursor molecule. Most likely, untimely entrapment of these nucleotides into the latter structure interferes with an ability of UTP24 to recognize the A_1 processing site, since it would be present in an improper structural context. Therefore, a highly conserved U3 snoRNA-18S rRNA interaction may play a comparable and essential role in processing at site A_1 in all eukaryotes.

In yeast, this interaction is also required for cleavage at site A_2, but not for processing at site A_0.[3, 4] On the contrary, in *Xenopus* oocytes U3 snoRNA the GAC element, box A', and 5'-terminal part of box A appear to play an important role in cleavage at site A_1 and processing at the 3'-end of the 18S rRNA segment, whereas box A is also important for processing at site A_0.[5] This difference may be due to the fact that unlike the situation in yeast (**Fig. S12A**), the 3'-terminal part of box A in *Xenopus* U3 snoRNA can potentially base-pair with five nucleotide sequence located in the 5'-ETS directly preceding the A_0 site (**Fig. S12C**). This species-specific interaction may position U3 snoRNA correctly on pre-rRNA to enable U3-dependent cleavage at the A_0 site in *Xenopus*.

In all organisms analyzed to date, box A' may interact either with nucleotides 18-21 of the 18S rRNA module, opposite site A_1, or with a sequence located several nucleotides upstream of the mature 18S rRNA 3'-end. These two base pairings, which are likely transient and mutually exclusive, were proposed to draw both ends of the 18S rRNA within the pre-rRNA precursor in close proximity (**Fig. S12A-D**). This suggests that U3 snoRNA bridges both termini of 18S to enable coordination of cleavage and temporal control of its maturation.[5]

The U3 snoRNA hinge region is involved in the formation of two duplexes with sequences within the 5'-ETS. Such interactions between the U3 snoRNA hinge and 5'-ETS region occur in all organisms analyzed to date and are believed to correctly position U3 snoRNA boxes A and A' relative to the pre-rRNA substrate for their functions in processing at U3-dependent sites. However, the detailed nature of these base-pairings is different in various species (**Fig. S12A-D**).

In yeast, the 5' terminal region of the U3 hinge (5'-hinge) hybridizes with the 5'-ETS site I,[6-8] which is located relatively close to the processing site A_0, and its 3'-terminal region (3'-hinge) contacts 5'-ETS site II that is localized further upstream of site I (**Fig. S12A**).[9, 10] Disruption of base-pairing between the U3 snoRNA 5'-hinge and 5'-ETS site I has long been known to block cleavages at sites A_0, A_1, and A_2.[6-8] It was postulated that it may promote targeting of an unknown endonuclease responsible for processing at site A_0.[4] In turn, the U3 snoRNA 3' hinge-5'-ETS site II interaction was relatively recently demonstrated to be a pre-requisite for U3 snoRNA 5'-hinge-5'-ETS site I base-pairing.[9, 10] Moreover, it is required for correct SSU processome assembly (in particular recruitment of Mpp10, Imp3, and Imp4 proteins) in *S. cerevisiae*.[9, 10] Both functions of

this interaction are most likely consequences of the fact that the 5'-ETS site II is the first one that becomes available for base-pairing with U3 snoRNA during rDNA transcription by RNA polymerase I.[9]

In *Xenopus* oocytes, the U3 snoRNA 5'-hinge and 3'-hinge base pair with two complementary 5'-ETS regions that are equivalent to the yeast sites I and II, respectively (**Fig. S12C**).[11, 12] In this organism, the U3 snoRNA 3'-hinge-5'-ETS site II interaction is more critical for 18S rRNA maturation.[12, 13] It was previously demonstrated to be indispensable for initial docking of U3 snoRNA on pre-rRNA, which may occur before transcription of the precursor has been completed.[11, 12] It was also found that the 5'-hinge and 3'-hinge have to be separated by a defined number of nucleotides to fulfill their function. Similarly, distances between the hinge region and boxes A/A' and between the U3 snoRNA 5'-end and box A are important for pre-rRNA processing.[5, 11]

It should be emphasized that one of the major characteristics distinguishing pre-rRNA processing in mammalian cells from that occurring in yeast is the presence of an additional cleavage site in the 5'-ETS, called A'. In this context, it is worth noting that in both *Trypanosoma* and mammalian cells, U3 snoRNA 3'-hinge interacts with the 5'-ETS site II localized much farther upstream of the A_0 processing site than in yeast and relatively near the 5'-end of 5'-ETS. In turn, this sequence is 3'-adjacent to the processing site A' (**Fig. S12B and S12D**).[14-16] Similar to cleavage at sites A_0, A_1, and A_2, processing at site A' is U3 snoRNA-dependent. It was suggested that the U3 snoRNA 3'-hinge base-pairing with 5'-ETS site II may influence the 5'-ETS structure and/or recruit a processing endonuclease, thus enabling cleavage at the neighboring site A'.[14] It is therefore plausible that the interaction between the U3 snoRNA 3'-hinge and 5'-ETS site II may be more important for processing at site A' than at site A_0 in the organisms, in which the former exists within pre-rRNA. Interestingly, while cleavage at site A' is a primary processing event in mammalian cells,[17] it does not play such an important function in *Trypanosoma* and rather does not occur at all in *Xenopus* oocytes.[18, 19] In the case of *Trypanosoma*, this may be due to significantly different interactions established between U3 snoRNA and pre-rRNA in a region surrounding the A' site, wherein the 3'-hinge seems to also interact with the counterpart of the yeast 5'-ETS site I, while the 5'-hinge most likely forms another base-pairing interactions, one of which directly involves the A' processing site (**Fig. S12B**).[18, 20] In turn, in the frog oocytes, the 5'-ETS site II hybridizes with the U3 snoRNA 3'-hinge much farther downstream of the 11 nucleotide

evolutionarily conserved motif (ECM) encompassing binding site for nucleolin (**Fig. S12C**), than in mouse, rat, and human 5'-ETS, where the two elements are adjacent to each other (**Fig. S12D**).[12] In vertebrates, the interaction of nucleolin with a conserved sequence within the ECM downstream of the potential A' processing site assists in docking of U3 snoRNA on the pre-rRNA substrate.[12, 21, 22] Since participation of the yeast nucleolin homolog in anchoring U3 snoRNA on pre-rRNA has not been demonstrated, this may explain why two interactions between both parts of the U3 snoRNA hinge and complementary 5'-ETS regions are essential for U3-dependent 18S rRNA maturation in *S. cerevisiae*, while in higher eukaryotes, most likely including humans, only U3 3'-hinge-site II base-pairing is critical, and the U3 5'-hinge-site I interaction plays an auxiliary role.[10] Although processing at site A' does not always take place, this RNA-protein interaction plays an important role in subsequent processing events leading to 18S rRNA maturation by promoting SSU processome assembly and stabilizing U3 snoRNA-pre-rRNA interactions.

Supplemental Figures

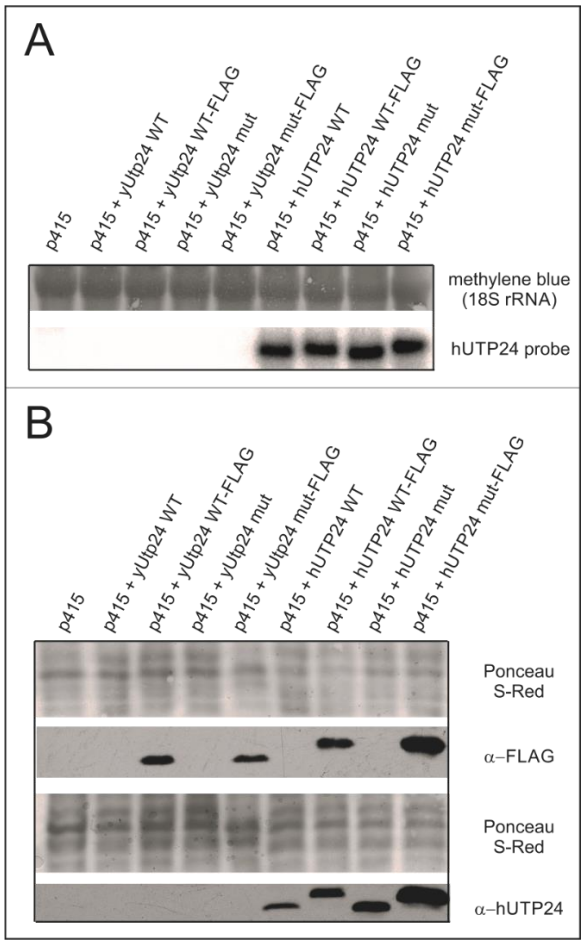

Figure S1. Analysis of expression of exogenous yUtp24 and hUTP24 in an *S. cerevisiae* strain with endogenous *yUTP24* under the control of doxycycline-repressible promoter, which was transformed with an empty p415 vector or its derivatives encoding WT or mut variants of yeast or human UTP24 proteins, bearing or lacking FLAG-tag at the C-terminus. (**A**) Exogenous transcripts encoding hUTP24 variants are present in the transformed yeast strains. Total RNA was isolated from the respective transformants and analyzed by northern blot with PCR probe corresponding to hUTP24 ORF. (**B**) Yeast and human UTP24 protein variants are efficiently produced in the transformed *S. cerevisiae* strains. Total protein extracts corresponding to the respective transformants were analyzed by western blot using antibodies against FLAG epitope or hUTP24 protein.

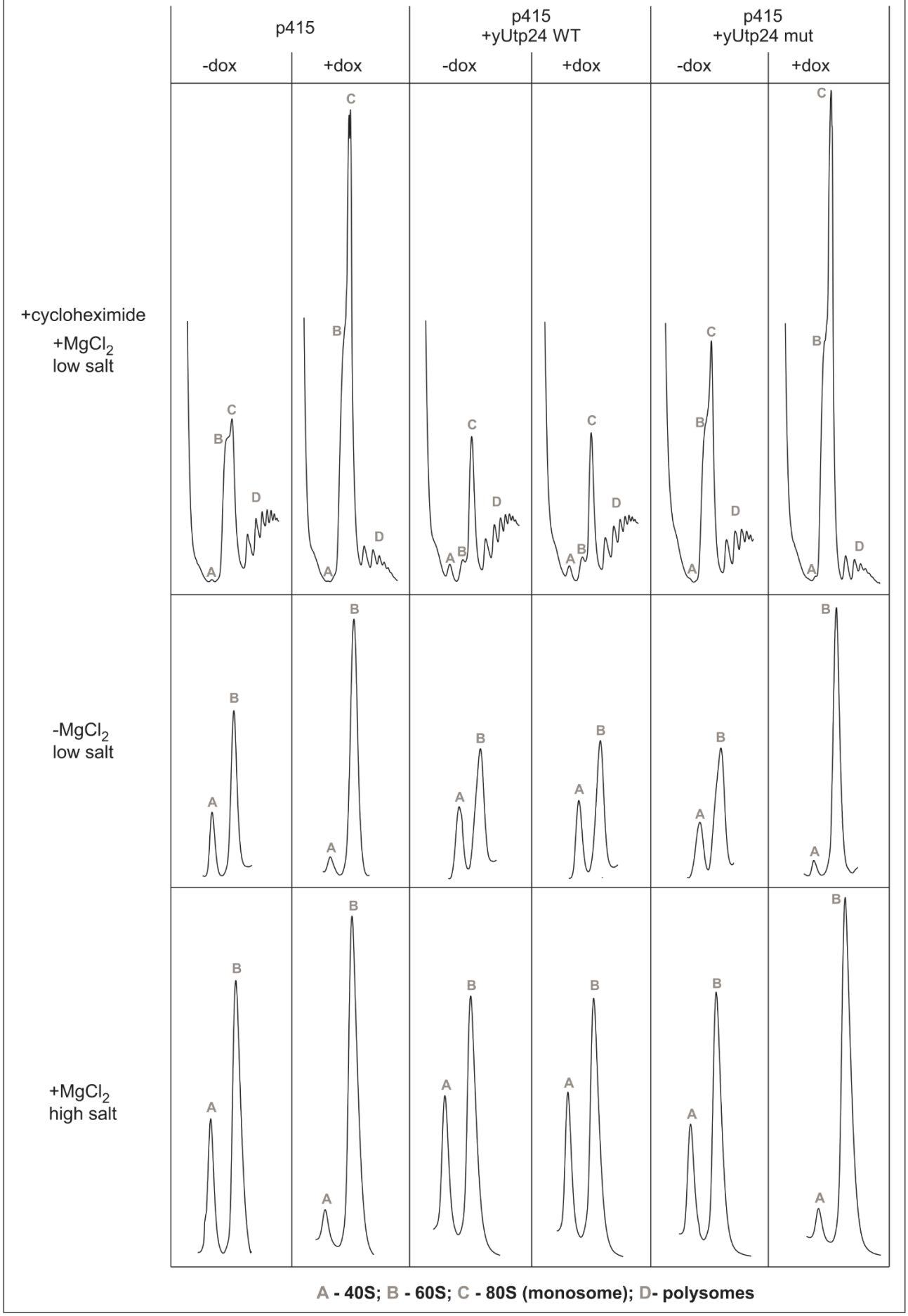
p415
-dox
+dox
p415
+yUtp24 WT
-dox
+dox
p415
+yUtp24 mut
-dox
+dox
+cycloheximide
+MgCl2
low salt
-MgCl2
low salt
+MgCl2
high salt
A
B
C
D
A - 40S; B - 60S; C - 80S (monosome); D- polysomes

Figure S2. Mutation in the putative active site of yUtp24 leads to reduction of 40S subunit and polysome levels. *S. cerevisiae* strain with endogenous *yUTP24* under the control of doxycycline-regulated promoter was transformed with an empty p415 vector (Ø) or its derivatives encoding WT or mut variants of yUtp24 or hUTP24. Native cytoplasmic extracts were prepared from transformants grown either in the absence ("-dox") or in the presence ("+dox") of doxycycline, using buffers with cycloheximide (*top panel*), lacking magnesium (*middle panel*) or containing salt at high concentration (*bottom panel*), and separated by centrifugation in linear sucrose gradients, allowing for analysis of polysome and ribosome subunits profiles. Graphs show distribution of absorbance at 254 nm from the top (left) to the bottom (right). Peaks corresponding to individual subunits (40S and 60S), monosomes (80S) and polysomes are indicated.

In the presence of cycloheximide we observed a modest reduction of the mature 40S subunit and a marked decrease in the amounts of polysomes, with a concomitant increase in the pool of free 60S subunit and monosomes, compared to cells producing yUtp24 WT (*upper panel*). To better assess the lower level of free 40S subunits, we analyzed cytoplasmic extracts prepared under conditions that promoted dissociation of ribosomal subunits: either by eliminating magnesium from the lysis buffer (*middle panel*) or by using a high ionic strength buffer (*bottom panel*). In both instances we were able to demonstrate that the ratio of 40S/80S was significantly diminished upon yUtp24 depletion and co-expression of the yUtp24 mut, which was due to reduction of the 40S pool and concomitant increase of 60S levels. Taken together, these results indicate that yUtp24 dysfunction results in decreased levels of small ribosomal subunits, which further leads to the reduced number of actively translating ribosomes.

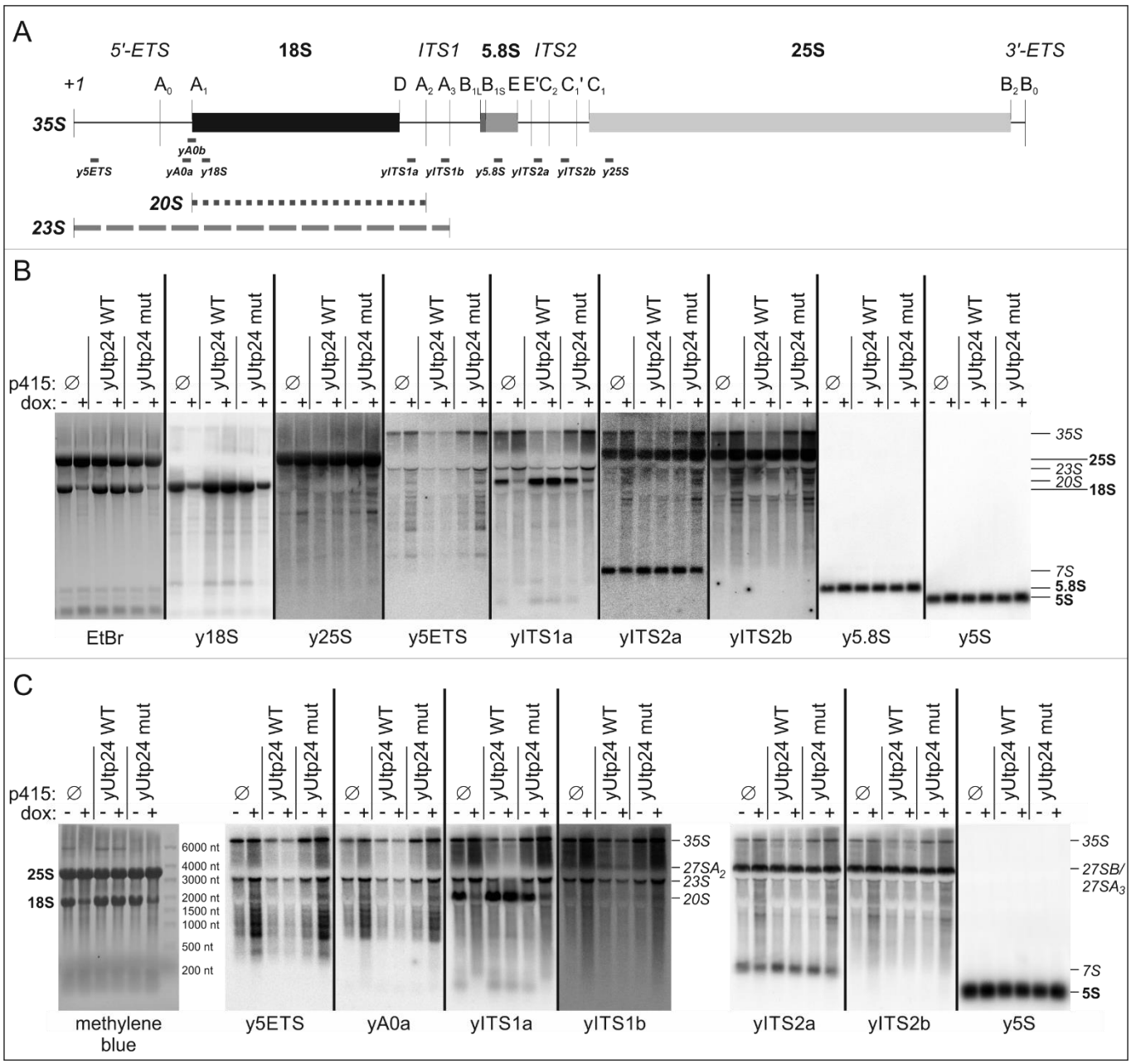

Figure S3. Northern blot analysis of pre-rRNA processing defects resulting from yUtp24 mutation. (**A**) A scheme of the *S. cerevisiae* 35S pre-rRNA. Positions of the processing sites within 35S precursor are indicated with vertical thin lines, along with the names. Nucleotide numbering is based on the GenBank 35S pre-rRNA sequence (accession number: BK006945.2). Grey bars below the primary 35S transcript show positions of oligonucleotides utilized as probes/primers in this study. Normal 20S precursor of 18S rRNA, extending from sites A_1 to A_2 is indicated with dotted line. Aberrant 23S species, resulting from inefficient processing at sites A_0, A_1 and A_2, extending from 5'-end of pre-rRNA to site A_3 is represented by a dashed line below 20S pre-rRNA. (**B**) *S. cerevisiae* strain with endogenous *yUTP24* under the control of doxycycline-regulated promoter was transformed with an empty p415 vector (Ø) or its derivatives encoding WT or mut variants of yUtp24. Total RNA was isolated from transformants grown either in

the absence ("dox: -") or in the presence ("dox: +") of doxycycline, separated in the denaturing agarose gel and transferred onto nylon membrane, which was then sequentially hybridized with probes complementary to different regions of 35S pre-rRNA, as indicated at the bottom. Positions of different RNA species are indicated on the right. The major visible phenotypes are: decreased levels of 18S rRNA and its natural precursor – 20S, and elevated levels of unprocessed 35S pre-rRNA as well as 23S intermediate. (**C**) The experiment was performed as in (B), but using additional probes (*yA0a* and *yITS1b*) in order to better demonstrate accumulation of 23S pre-rRNA.

A significant decrease of mature 18S rRNA levels, but not of 7S pre-rRNA and 5.8S or 25S rRNA, was observed for strains with UTP24 dysfunction (**panel B**). We also observed increased levels of 35S pre-rRNA, indicating a defect during the early processing steps (**panels B and C**). Hybridization with a probe targeting ITS1 between the 3'-end of 18S rRNA and processing site A_2 revealed a marked reduction of 20S rRNA (**panel B**), a stable 18S rRNA precursor extending from site A_1 to A_2 (**panel A**), which is converted into mature 18S rRNA by endonucleolytic cleavage at site D in the cytoplasm by the PIN-domain endonuclease Nob1. Experiments with probes targeting different parts of ITS1 and 5'-ETS revealed accumulation of a larger RNA species, 23S rRNA (**panels B and C**), which corresponds to the region from the transcriptional start site to processing site A_3 (**panel A**). These phenotypes confirmed the importance of yUtp24 for 18S rRNA maturation and indicate that its putative endoribonucleolytic activity is indispensable for U3 snoRNA-dependent processing events at sites A_0, A_1, and A_2.

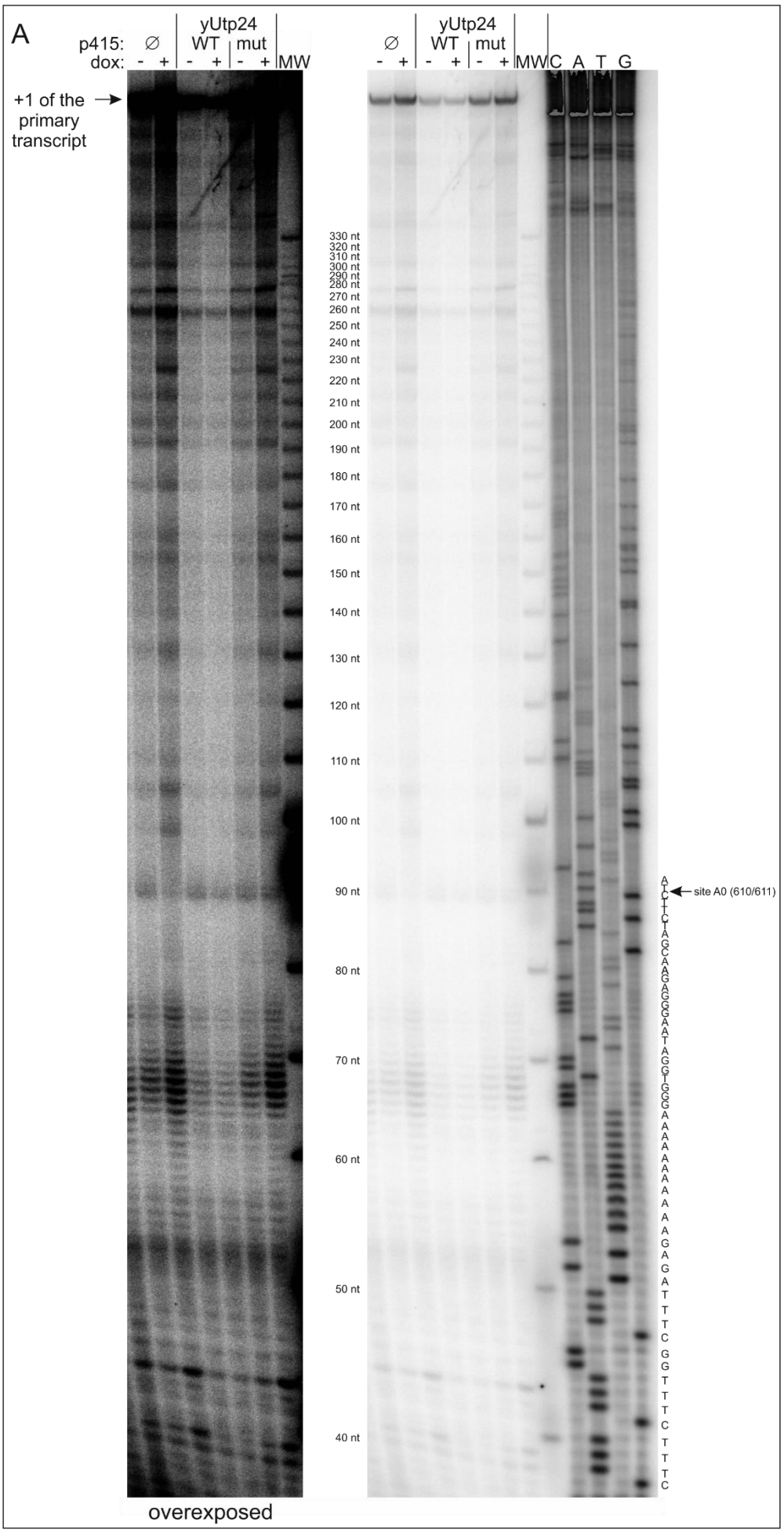
A
p415: ∅ yUtp24 WT mut
dox: - + - + - + MW
+1 of the primary transcript
330 nt
320 nt
310 nt
300 nt
290 nt
280 nt
270 nt
260 nt
250 nt
240 nt
230 nt
220 nt
210 nt
200 nt
190 nt
180 nt
170 nt
160 nt
150 nt
140 nt
130 nt
120 nt
110 nt
100 nt
90 nt
80 nt
70 nt
60 nt
50 nt
40 nt
∅ yUtp24 WT mut
- + - + - + MW C A T G
site A0 (610/611)
overexposed

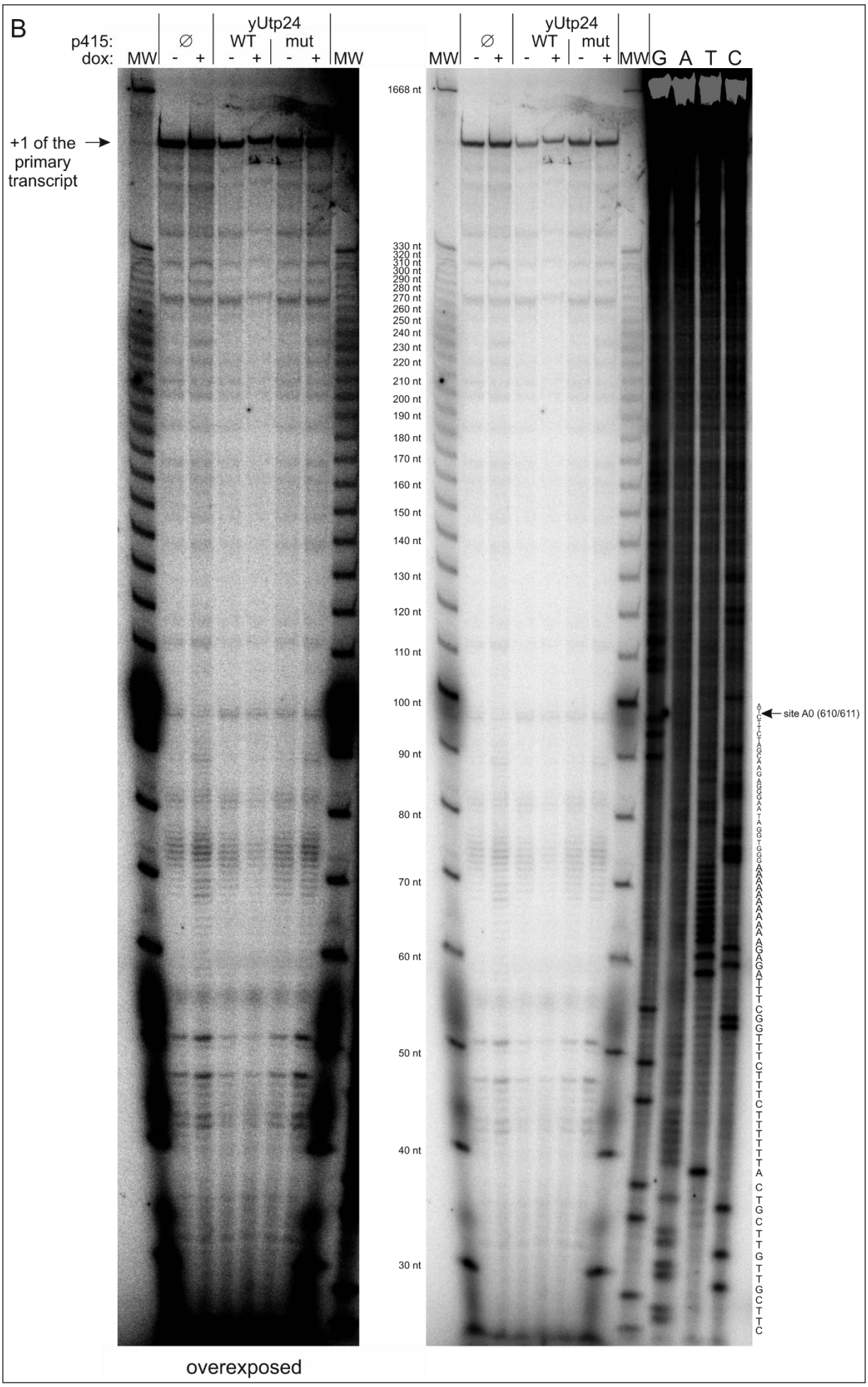
B
p415:
dox:
MW
∅
yUtp24
WT
mut
G A T C
+1 of the primary transcript
1668 nt
330 nt
320 nt
310 nt
300 nt
290 nt
280 nt
270 nt
260 nt
250 nt
240 nt
230 nt
220 nt
210 nt
200 nt
190 nt
180 nt
170 nt
160 nt
150 nt
140 nt
130 nt
120 nt
110 nt
100 nt
90 nt
80 nt
70 nt
60 nt
50 nt
40 nt
30 nt
site A0 (610/611)
overexposed

Figure S4. Primer extension analysis of yeast pre-rRNA processing at site A_0. Total RNA was isolated from *S. cerevisiae* strain with endogenous *yUTP24* under the control of doxycycline-regulated promoter, transformed with an empty p415 vector (Ø) or its derivatives encoding WT or mut variants of yUtp24, grown either in the absence ("-dox") or presence ("+dox") of doxycycline, and subjected to primer extension using oligonucleotides yA0a (**A**) or yA0b (**B**), hybridizing upstream of the site A_0. In both cases, the respective primer was used in parallel with a DNA template comprising an appropriate rDNA fragment to generate dideoxynucleotide sequencing ladders, which were co-electrophoresed with primer extension products. The retrieved sequences (in reverse complement) are presented next to the sequencing results. A 5'-end labeled DNA molecular weight marker (MW) was also run in parallel – sizes of the MW fragments are indicated next to the bands. Predicted positions of the A_0 site are indicated on the right. Bands corresponding to reverse transcription stops at the nucleotide +1 of the primary 35S transcript are indicated on the left.

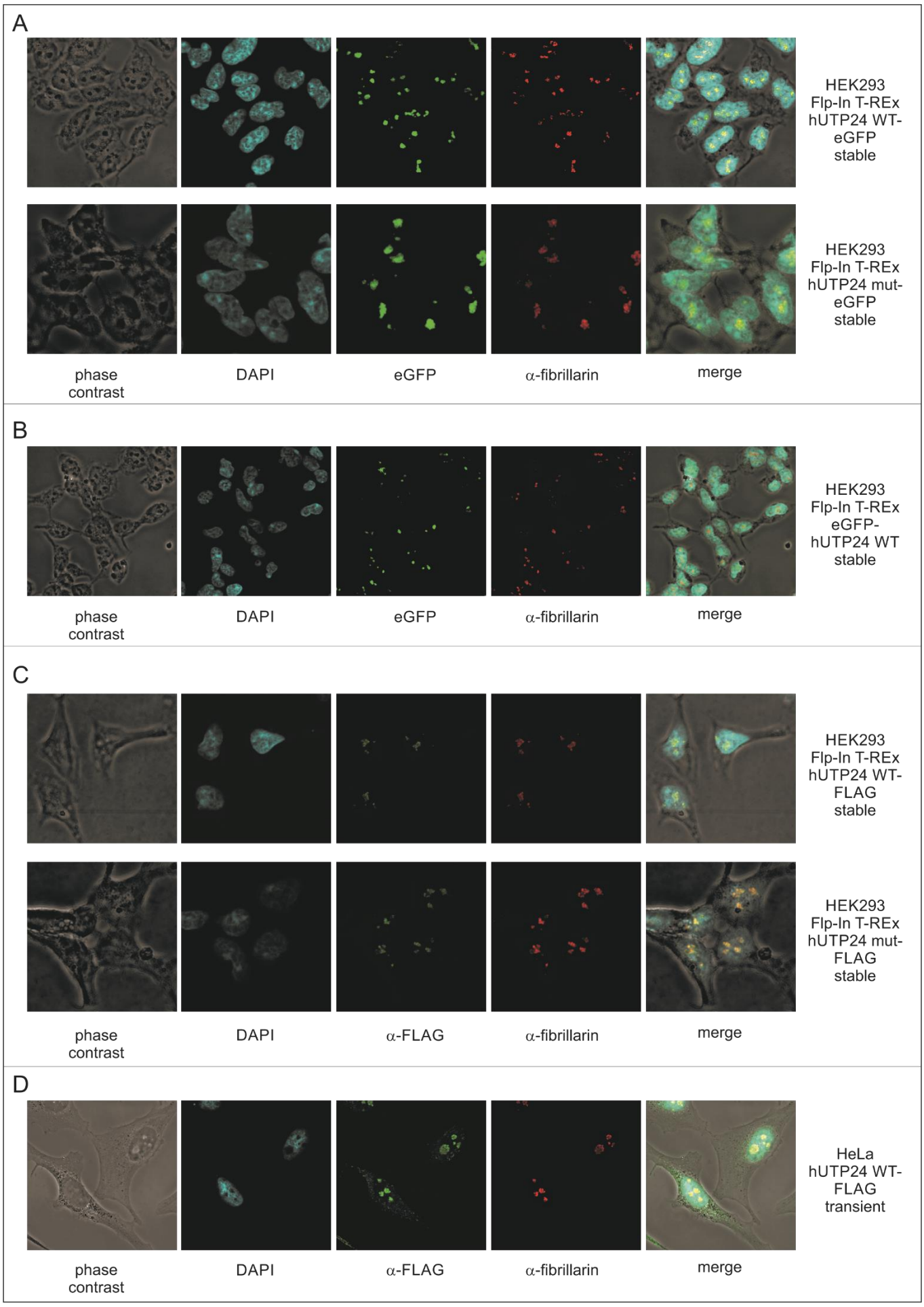
A
HEK293 Flp-In T-REx hUTP24 WT-eGFP stable
HEK293 Flp-In T-REx hUTP24 mut-eGFP stable
phase contrast
DAPI
eGFP
α-fibrillarin
merge
B
HEK293 Flp-In T-REx eGFP-hUTP24 WT stable
phase contrast
DAPI
eGFP
α-fibrillarin
merge
C
HEK293 Flp-In T-REx hUTP24 WT-FLAG stable
HEK293 Flp-In T-REx hUTP24 mut-FLAG stable
phase contrast
DAPI
α-FLAG
α-fibrillarin
merge
D
HeLa hUTP24 WT-FLAG transient
phase contrast
DAPI
α-FLAG
α-fibrillarin
merge

Figure S5. hUTP24 is localized in the nucleoli of human cells. (**A**) Stable HEK293 Flp-In T-REx cell lines bearing exogenous sequences coding for C-terminally eGFP-tagged hUTP24 WT or mut were subjected to induction with doxycycline. Immunofluorescence was then performed using anti-fibrillarin (nucleolar marker) antibodies (detected with secondary antibodies coupled with Alexa Fluor 555 fluorescent dye), in combination with DAPI staining of the nuclei. (**B**) Stable HEK293 Flp-In T-REx cell line producing hUTP24 WT with eGFP N-terminus upon doxycycline-mediated induction was subjected to immunofluorescence as in (A). (**C**) Stable HEK293 Flp-In T-REx cell lines producing C-terminally FLAG-tagged hUTP24 WT or mut were subjected to immunofluorescence using anti-FLAG and anti-fibrillarin (nucleolar marker) antibodies (detected with secondary antibodies coupled with Alexa Fluor 488 and 555 fluorescent dyes, respectively); nuclei were stained with DAPI. (**D**) HeLa cells were transiently transfected with construct encoding hUTP24 WT-FLAG fusion and subjected to immunofluorescence as in (C). In all cases signals from FLAG/eGFP and fibrillarin co-localized in the nucleoli.

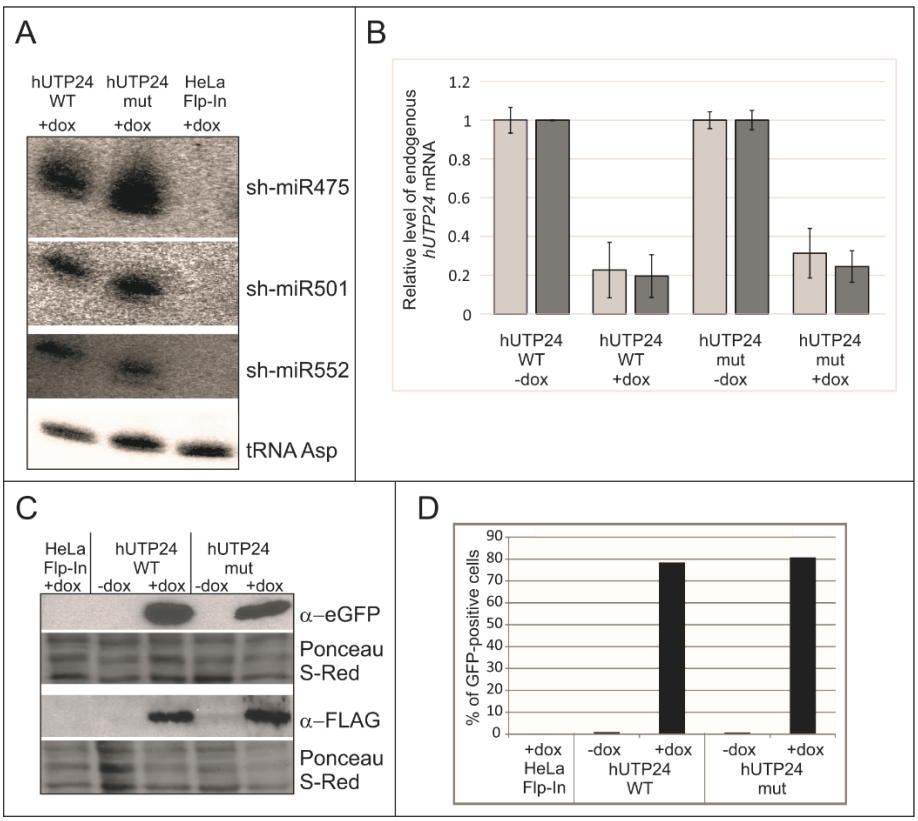

Figure S6. Validation of the human model cell lines co-expressing sh-miRNA downregulating endogenous *hUTP24* and exogenous sh-miRNA-insensitive exogenous copy of wild-type or mutant hUTP24. (**A**) All three sh-miRNA targeting various sites in the endogenous *hUTP24* mRNA were synthesized following doxycycline-mediated induction of expression in cells stably transfected with the relevant plasmid constructs, but not in the parental HeLa Flp-In T-REx cell line. Total RNA was isolated from the indicated cell lines treated with doxycycline and analyzed by northern blot with oligo probes complementary to each of the sh-miRNA. tRNA Asp was employed as a loading control. (**B**) sh-miRNA efficiently downregulate expression of endogenous *hUTP24* at the mRNA level. Quantitative PCR analysis was performed on total RNA isolated from the model cell lines grown in the absence of doxycycline ("-dox") or subjected to induction ("+dox"), using two different primer pairs (represented by light- or dark-grey rectangles) complementary to hUTP24. The graph shows results of quantification of three independent experiments. GAPDH mRNA was used for normalization. The expression level is relative to the untreated cell line with hUTP24 WT. The level of endogenous *hUTP24* mRNA decreased to approximately 20-30% upon induction (depending on the primer pair employed), compared to the non-induced cells. (**C**) eGFP and exogenous hUTP24 variants are expressed in the model cell lines following induction. Total protein extracts were prepared from the indicated cell lines, either untreated ("-dox") or treated ("+dox") with doxycycline and analyzed by western blot

using anti-eGFP or anti-FLAG antibodies. Ponceau S-Red staining of the nitrocellulose membrane following protein transfer was used as a loading control. (**D**) FACS analysis of eGFP level in the parental HeLa Flp-In T-REx cell line and the model cell lines established in this study, grown in a medium without doxycycline ("-dox") or in the presence ("+dox") of inducer. Synthesis of eGFP from the co-cistron with sh-miRNA was specifically induced in the model cell lines, demonstrating that our experimental system appeared to be relatively tight, as the number of eGFP-positive cells in the absence of the inducer was comparable to that of the background from a non-transfected HeLa Flp-In T-Rex line.

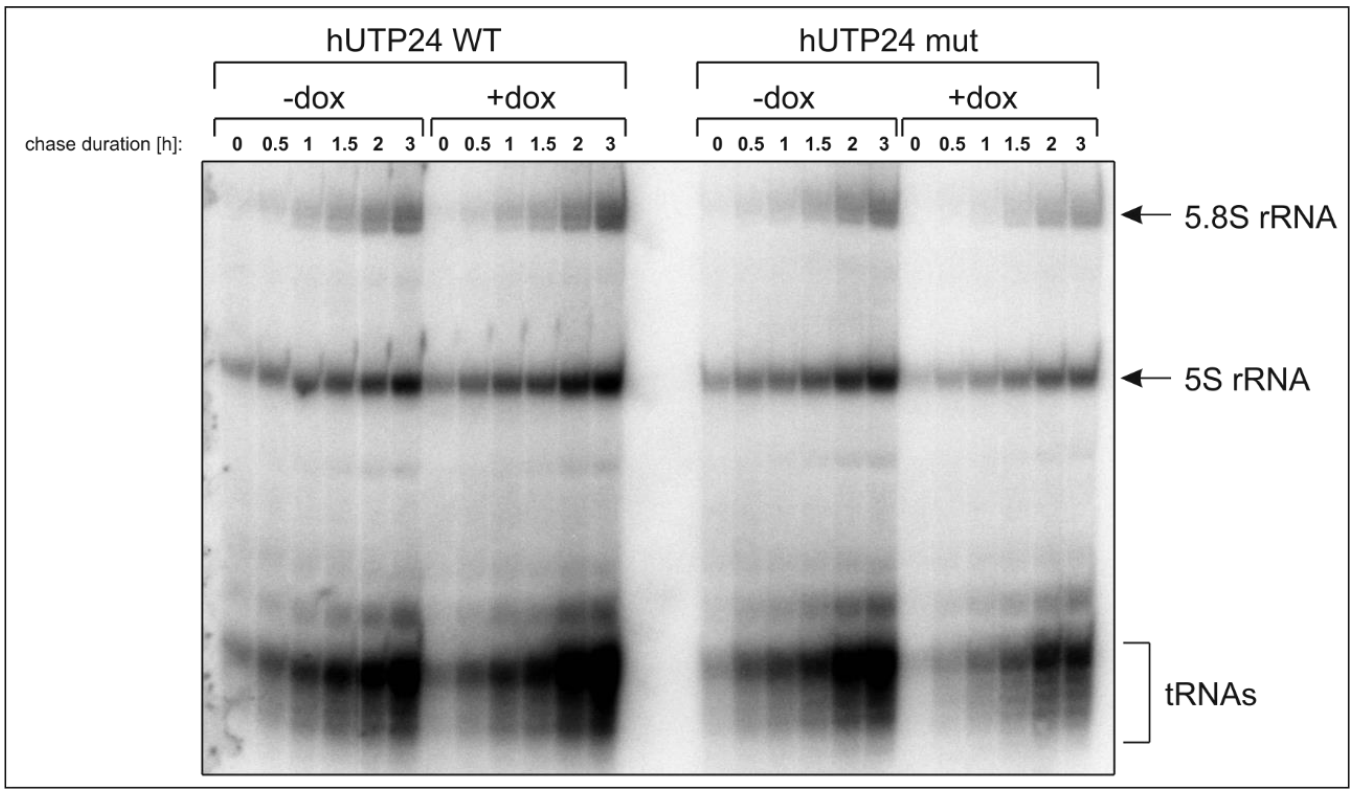

Figure S7. Mutation in the putative active site of hUTP24 does not significantly influence *de novo* synthesis of 5.8S and 5S rRNA. Model cell lines cultured in a medium lacking doxycycline ("-dox") or in the presence of inducer ("+dox") were pulse labeled with ^{32}P orthophosphoric acid, followed by chase in normal media for varying times (indicated above each lane). RNA was isolated from the cells, separated in denaturing polyacrylamide gel and transferred onto nylon membrane, which was subjected to phosphorimaging. Positions of 5.8S and 5S rRNA as well as tRNAs are indicated with on the right.

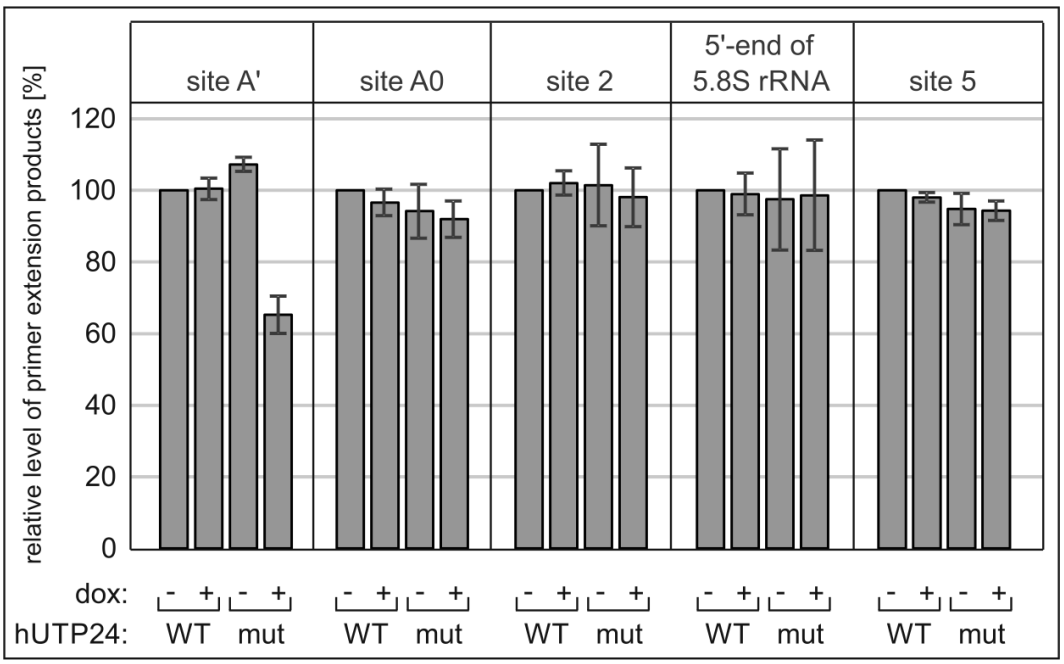

Figure S8. Quantification of the results of primer extension experiments performed using total RNA isolated from model cell lines producing either wild-type (WT) or mutant (mut) hUTP24, either untreated ("dox: -") or treated with doxycycline ("dox: +") (related to **Fig. 10** in the main text). The graphs represent mean values (fold changes of the amounts of primer extension products relative to the cell line with wild-type hUTP24, not subjected to induction with doxycycline) of three independent experiments. 5S rRNA levels assessed by northern blot using the same amounts of total RNA as employed in primer extension experiments (see **Fig. 9B** for an example), were used for normalization. Error bars reflect standard deviation.

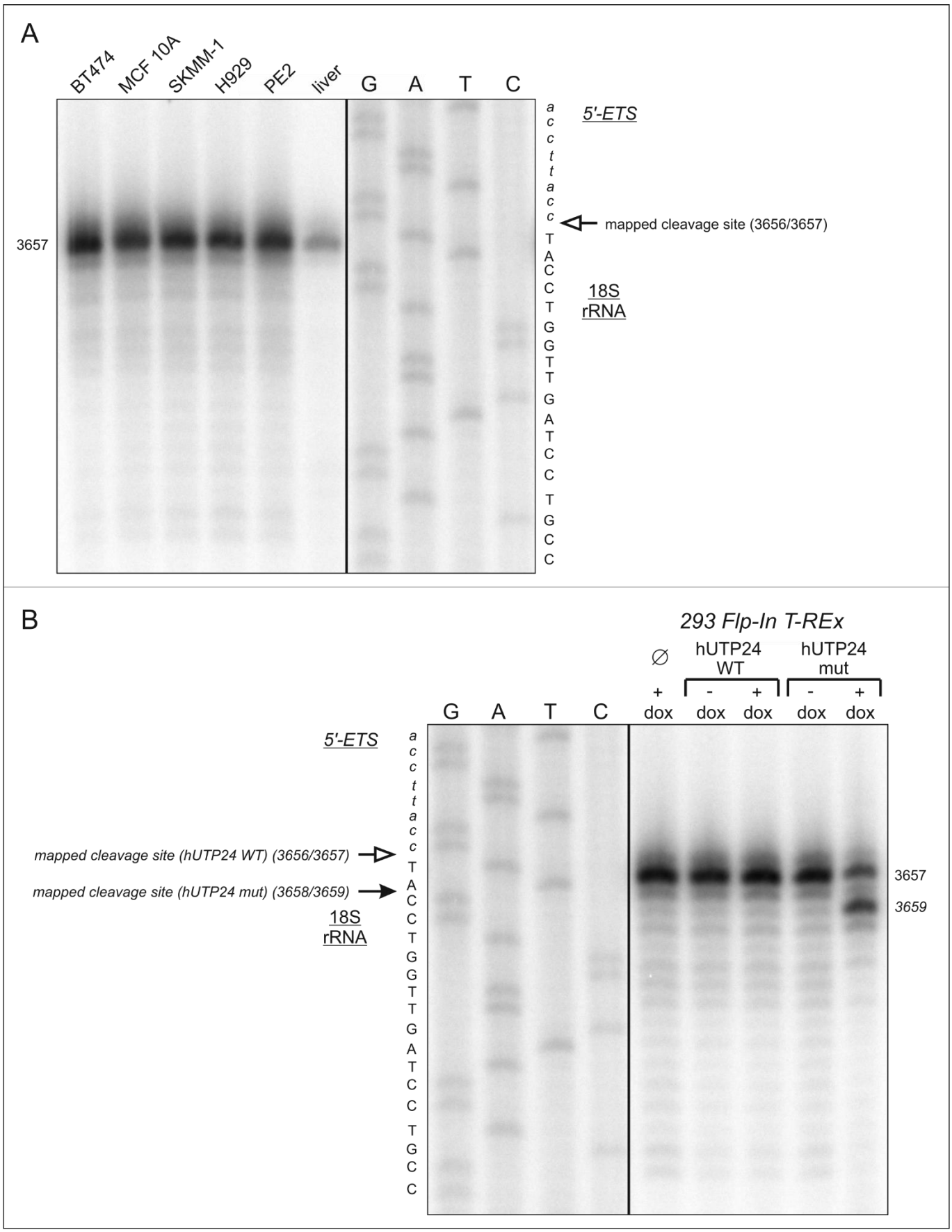
A
BT474
MCF 10A
SKMM-1
H929
PE2
liver
G
A
T
C
3657
5'-ETS
a c c t t a c c T A C C T G G T T G A T C C T G C C
mapped cleavage site (3656/3657)
18S rRNA
B
293 Flp-In T-REx
∅
hUTP24 WT
hUTP24 mut
+
-
+
-
+
dox
dox
dox
dox
dox
G
A
T
C
5'-ETS
mapped cleavage site (hUTP24 WT) (3656/3657)
mapped cleavage site (hUTP24 mut) (3658/3659)
18S rRNA
3657
3659

Figure S9. Analysis of pre-rRNA processing at site A_1 in human cells from different sources. Primer extension experiment was performed on total RNA isolated from human cell lines derived from the mammary gland (BT474, MCF 10A), multiple myeloma cell lines (SKMM-1, H929, PE2) and human liver (**A**) or from HEK293 Flp-In T-REx and its derivatives co-expressing sh-miRNA downregulating endogenous *hUTP24* and exogenous sh-miRNA-insensitive exogenous copy of wild-type or mutant hUTP24 (**B**), grown either in the absence ("-dox") or presence ("+dox") of doxycycline. Note that much lower intensity of the band observed in a lane corresponding to the liver sample is due to the fact that only 600 ng (instead of 4 μg) of RNA was used for reverse transcription. The same primer was employed in parallel with DNA template comprising appropriate rDNA fragment to generate dideoxynucleotide sequencing ladders, which were co-electrophoresed with primer extension products. Retrieved sequence (in reverse complement) is presented next to the sequencing results. In most cases, cleavage site was mapped between nucleotides 3656 and 3657 in 47S pre-rRNA. Only in cells producing mutant variant of hUTP24, the major reverse transcription stop was shifted 2 nucleotides downstream.

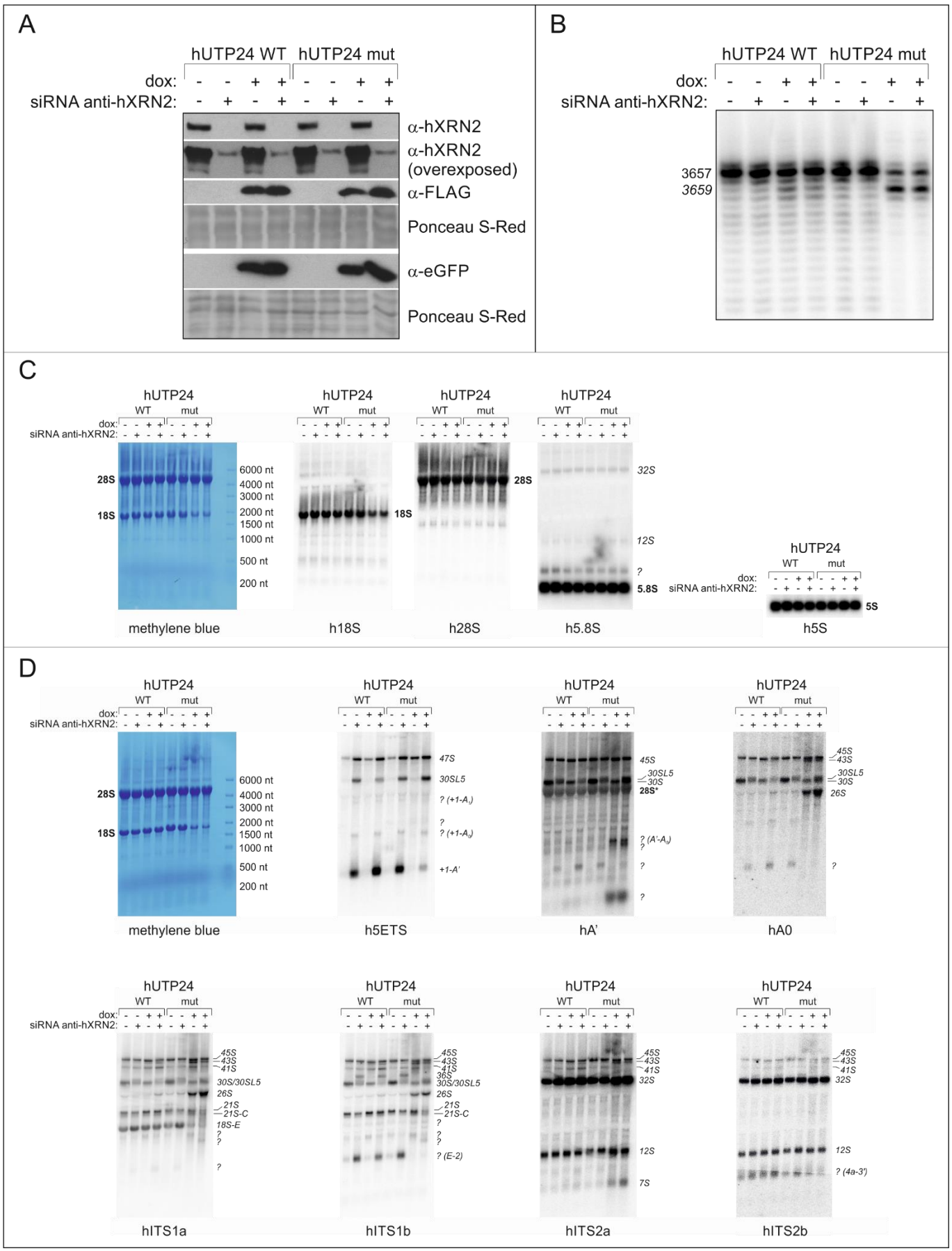
A
hUTP24 WT
hUTP24 mut
dox:
siRNA anti-hXRN2:
α-hXRN2
α-hXRN2 (overexposed)
α-FLAG
Ponceau S-Red
α-eGFP
Ponceau S-Red
B
hUTP24 WT
hUTP24 mut
dox:
siRNA anti-hXRN2:
3657
3659
C
hUTP24
WT
mut
dox:
siRNA anti-hXRN2:
28S
18S
6000 nt
4000 nt
3000 nt
2000 nt
1500 nt
1000 nt
500 nt
200 nt
32S
12S
?
5.8S
5S
methylene blue
h18S
h28S
h5.8S
h5S
D
hUTP24
WT
mut
dox:
siRNA anti-hXRN2:
28S
18S
6000 nt
4000 nt
3000 nt
2000 nt
1500 nt
1000 nt
500 nt
200 nt
47S
30SL5
? (+1-A1)
?
? (+1-A0)
+1-A'
45S
30SL5
30S
28S*
? (A'-A0)
?
?
?
45S
43S
30SL5
30S
26S
?
methylene blue
h5ETS
hA'
hA0
45S
43S
41S
30S/30SL5
26S
21S
21S-C
18S-E
?
?
?
45S
43S
41S
36S
30S/30SL5
26S
21S
21S-C
?
?
?
? (E-2)
45S
43S
41S
32S
12S
7S
45S
43S
41S
32S
12S
? (4a-3')
hITS1a
hITS1b
hITS2a
hITS2b

Figure S10. Knockdown of *hXRN2* expression does not influence pre-rRNA processing defects resulting from hUTP24 mutation. (**A**) Western blot analysis for protein samples from model cell lines untreated ("dox: -") or treated ("dox: +") with doxycycline, which were transfected with either siRNA against hXRN2 ("siRNA anti-hXRN2: +") or with control, unrelated siRNA ("siRNA anti-hXRN2: -"); following transfer of proteins separated in SDS-PAGE onto nitrocellulose membrane, it was probed with antibodies specific to hXRN2, FLAG epitope or eGFP; staining of the membrane with Ponceau S Red was employed as a loading control. (**B**) Analysis of pre-rRNA processing at site A_1. Primer extension was performed on total RNA isolated from model human cell lines described in (A). (**C**) Northern blot analysis of the mature rRNA levels. Total RNA was isolated from model cell lines described in (A), separated in the denaturing agarose-formaldehyde gel and transferred onto nylon membrane, which was then stained with methylene blue and sequentially hybridized with probes complementary to mature rRNA, as indicated at the bottom. Positions of different RNA species are indicated on the right. (**D**) Northern blot analysis of the pre-rRNA processing intermediates. Experiment was performed as in (B), but employing probes targeting various regions of 5'-ETS, ITS1 and ITS2, as indicated at the bottom. Positions of different RNA species are indicated on the right.

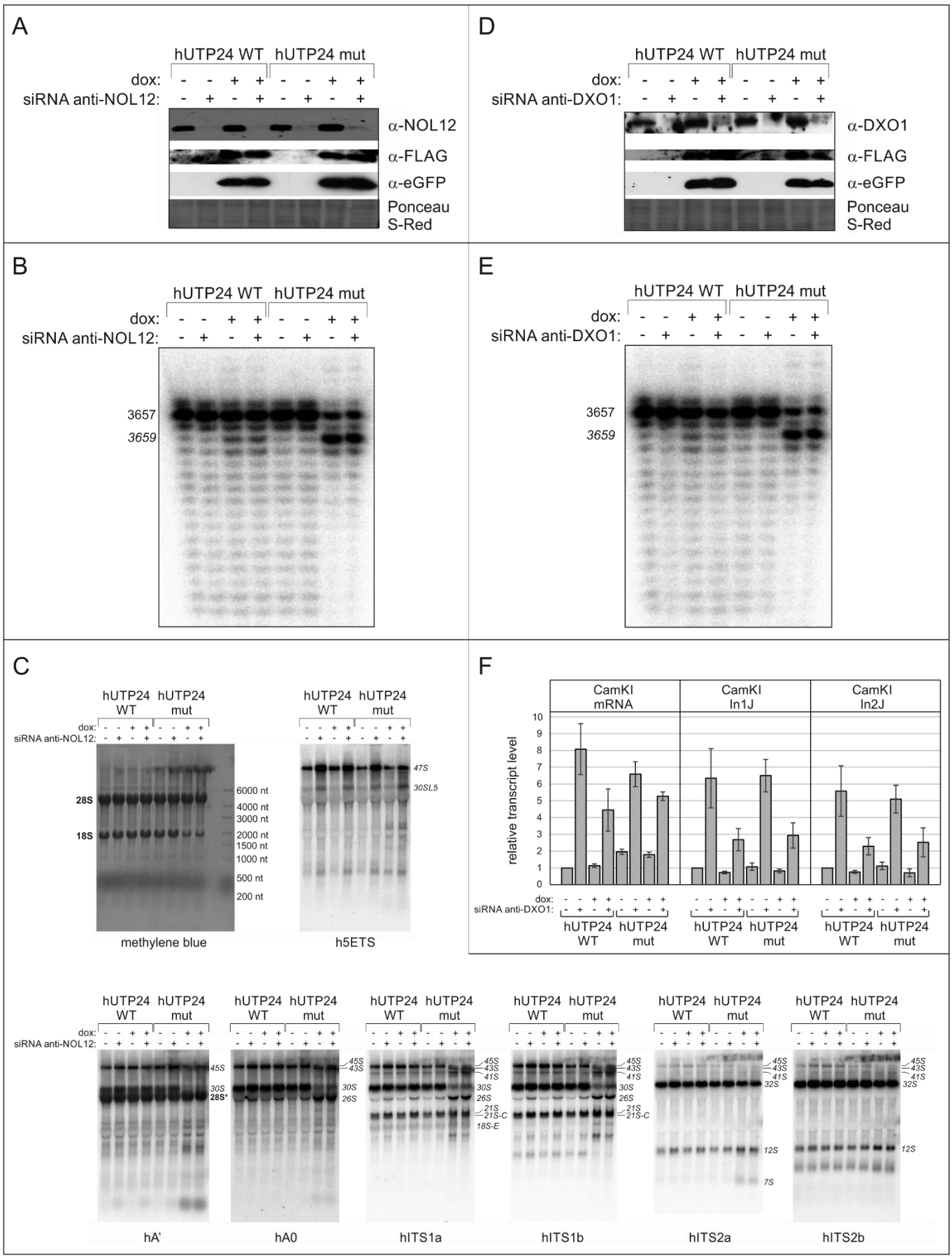
A
hUTP24 WT
hUTP24 mut
dox:
siRNA anti-NOL12:
α-NOL12
α-FLAG
α-eGFP
Ponceau S-Red
D
hUTP24 WT
hUTP24 mut
dox:
siRNA anti-DXO1:
α-DXO1
α-FLAG
α-eGFP
Ponceau S-Red
B
hUTP24 WT
hUTP24 mut
dox:
siRNA anti-NOL12:
3657
3659
E
hUTP24 WT
hUTP24 mut
dox:
siRNA anti-DXO1:
3657
3659
C
hUTP24 WT
hUTP24 mut
dox:
siRNA anti-NOL12:
28S
18S
6000 nt
4000 nt
3000 nt
2000 nt
1500 nt
1000 nt
500 nt
200 nt
methylene blue
47S
30SL5
h5ETS
F
CamKI mRNA
CamKI In1J
CamKI In2J
relative transcript level
dox:
siRNA anti-DXO1:
hUTP24 WT
hUTP24 mut
hA'
hA0
hITS1a
hITS1b
hITS2a
hITS2b
45S
43S
41S
32S
30S
28S*
26S
21S
21S-C
18S-E
12S
7S

Figure S11. Aberrant processing at site A_1, observed upon hUTP24 dysfunction, is not due to the 5'-3' exoribonucleolytic activities of NOL12 or DXO1. (**A**) Model cell lines were either untreated ("dox: -") or treated ("dox: +") with doxycycline, and transfected with siRNA against NOL12 ("siRNA anti-NOL12: +") or with control, unrelated siRNA ("siRNA anti-NOL12: -"); proteins extracted from cells were separated in SDS-PAGE and transferred onto nitrocellulose membrane, which was probed sequentially with antibodies specific to NOL12, FLAG epitope or eGFP; staining of the membrane with Ponceau S Red was employed as a loading control. (**B**) pre-rRNA processing at site A_1 was analysed by primer extension performed on total RNA isolated from the same cells as in (A). (**C**) Northern blot analysis of the pre-rRNA processing intermediates. Total RNA was isolated from model cell lines described in (A), separated in the denaturing agarose-formaldehyde gel and transferred onto nylon membrane, which was then stained with methylene blue and sequentially hybridized with probes complementary to different regions of 5'-ETS, ITS1 and ITS2, as indicated at the bottom. Positions of different RNA species are indicated on the right. (**D**) Experiment was performed as in (A), but employing siRNA against DXO1 and antibodies specific to this protein. (**E**) pre-rRNA processing at site A_1 was analysed by primer extension performed on total RNA isolated from the same cells as in (D). (**F**) Quantitative RT-PCR analysis of CamKI mature mRNA and pre-mRNA (containing unspliced intron 1 or intron 2) levels on total RNA isolated from the same cells as in (D). The graphs show results of quantification of three independent experiments; values on the left represent fold change in the level of transcript relative to the cell line with wild-type hUTP24, not subjected to induction by doxycycline and treated with control siRNA, which was arbitrarily set to 1. GAPDH mRNA was used for normalization in all cases.

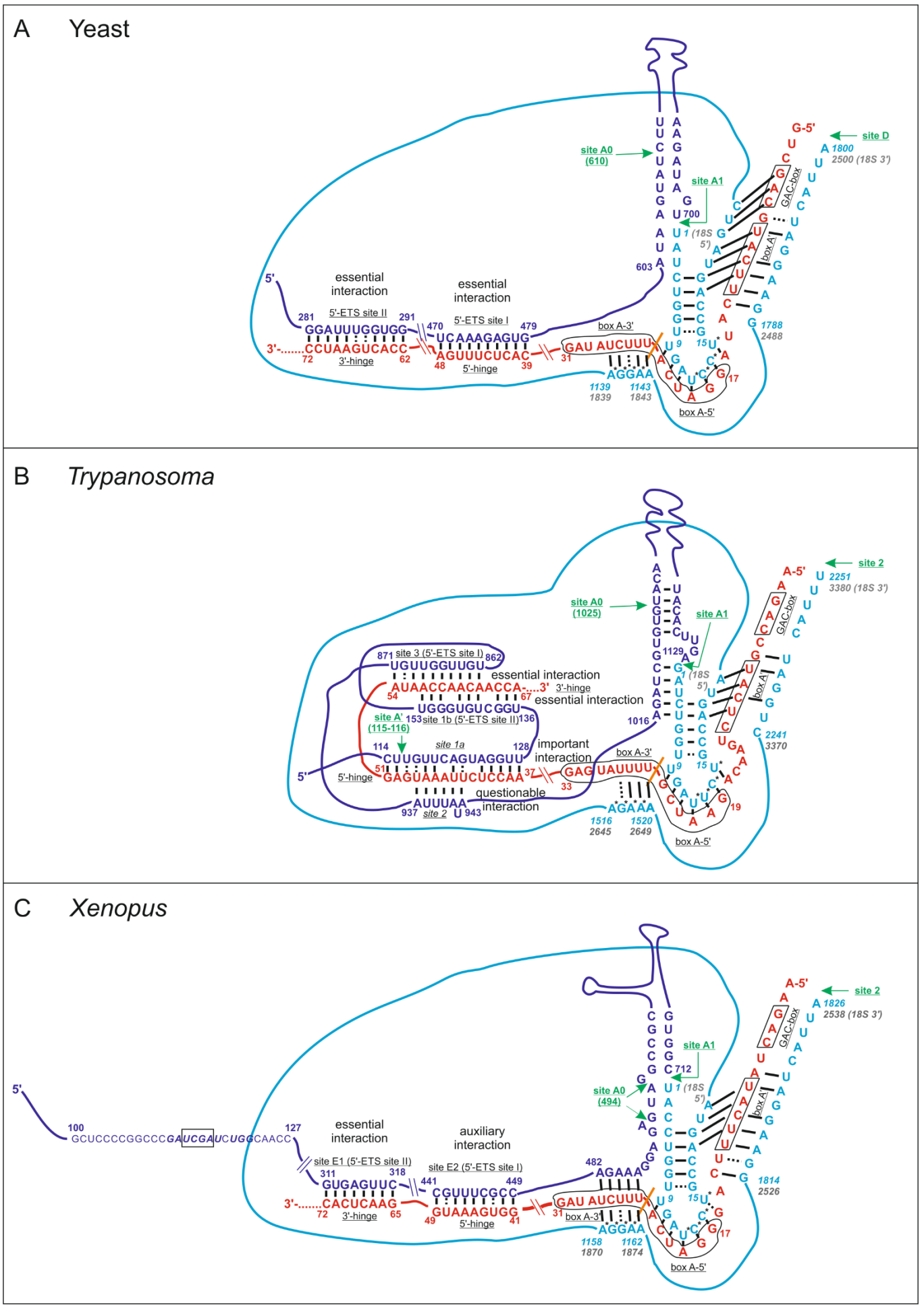
A Yeast
site A0 (610)
site A1
site D
G-5'
A 1800
2500 (18S 3')
GAC-box
box A'
1 (18S 5')
700
603
5'
essential interaction
5'-ETS site II
281
291
GGAUUUGGUGG
3'-.....CCUAAGUCACC
72
3'-hinge
62
essential interaction
5'-ETS site I
470
479
UCAAAGAGUG
AGUUUCUCAC
48
5'-hinge
39
box A-3'
GAU AUCUUU
31
9
15
17
AGGAA
1139
1839
1143
1843
box A-5'
1788
2488
B Trypanosoma
site A0 (1025)
site A1
site 2
A-5'
U 2251
3380 (18S 3')
GAC-box
box A'
1 (18S 5')
1129
1016
871
site 3 (5'-ETS site I)
862
UGUUGGUUGU
essential interaction
AUAACCAACAACCA-....3'
3'-hinge
54
67
essential interaction
UGGGUGUCGGU
site A'
(115-116)
153
site 1b (5'-ETS site II)
136
114
site 1a
128
important interaction
CUUGUUCAGUAGGUU
5'
5'-hinge
51
GAGUAAAUUCUCCAA
37
questionable interaction
AUUUAA
937
site 2
U 943
box A-3'
GAG UAUUUU
33
9
15
19
AGAAA
1516
2645
1520
2649
box A-5'
2241
3370
C Xenopus
site A0 (494)
site A1
site 2
A-5'
A 1826
2538 (18S 3')
GAC-box
box A'
1 (18S 5')
712
5'
100
GCUCCCCGGCCCGAUCGAUCUGGCAACC
127
essential interaction
auxiliary interaction
site E1 (5'-ETS site II)
311
318
GUGAGUUC
3'-.....CACUCAAG
72
3'-hinge
65
site E2 (5'-ETS site I)
441
449
CGUUUCGCC
GUAAAGUGG
49
5'-hinge
41
482
AGAAA
box A-3'
GAU AUCUUU
31
9
15
17
AGGAA
1158
1870
1162
1874
box A-5'
1814
2526

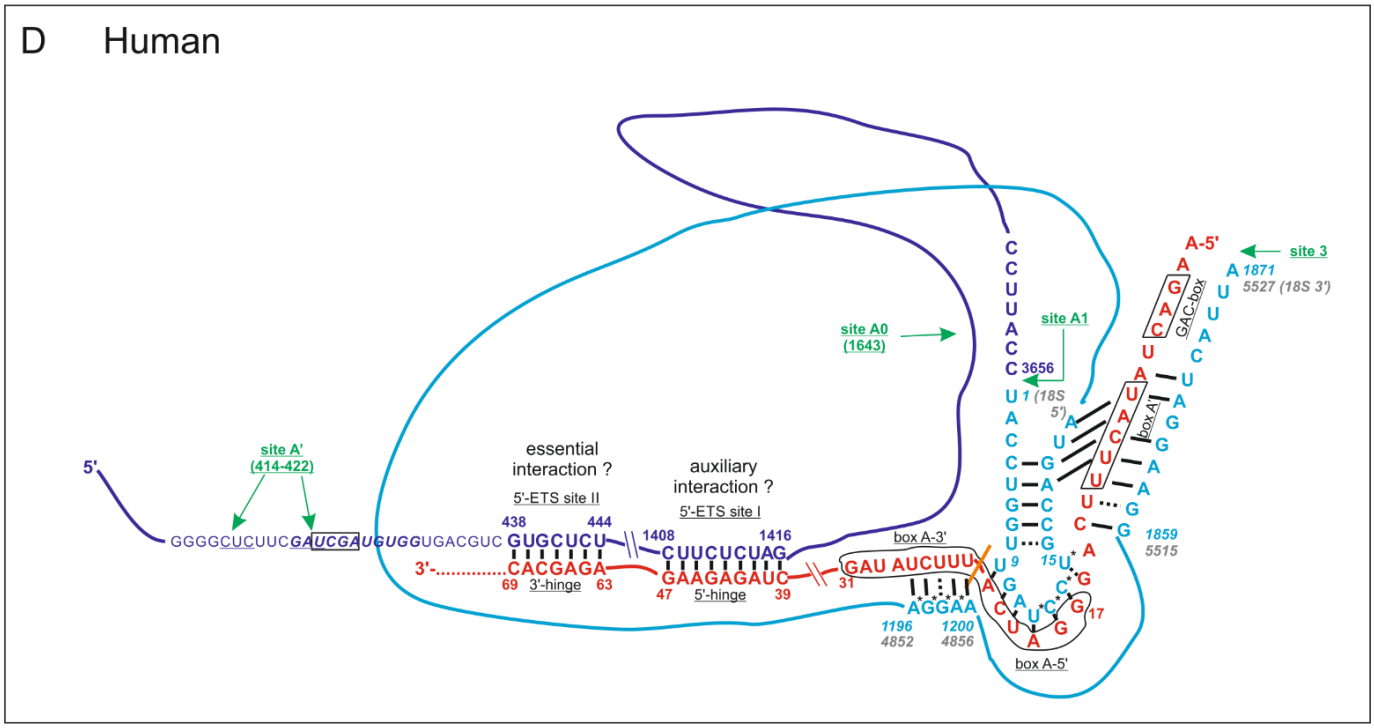

Figure S12. Schemes of interactions between U3 snoRNA and pre-rRNA in yeast (**A**), *Xenopus* oocytes (**B**), *Trypanosoma brucei* (**C**) and human cells (**D**) (based on ref. 24). U3 snoRNA molecules are depicted in red; positions of key functional elements (GAC-box, box A', box A, 5'-hinge and 3'-hinge) are indicated; 5'-ETS is drawn in dark blue and 18S rRNA fragments – in light blue; nucleotides in 18S rRNA involved in the formation of a central pseudoknot, which is prevented by their base-pairing with 5'-terminal and 3'-terminal parts of U3 snoRNA boxA (box A-5'/box A-3'), are indicated with asterisks; orange lines schematically separate 5' and 3' parts of the U3 snoRNA box A; positions of cleavage sites (shown in green) are marked with arrows; 11-nt-long evolutionary conserved motives (ECM) in the 5'-ETS of *Xenopus* and human pre-rRNA are bolded and italicized; nucleolin-binding sites are indicated with rectangles; numbering in grey represents nucleotide positioning with respect to the first base of pre-rRNA molecule.

GAATTCATATAGTCGACCAGTGGATCCTGGAGGCTTGCTGAAGGCTGTATGCTGTTTCAGGTCCCGGTCA

ACTGTGTTTTGGCCACTGACTGACACAGTTGAGGGACCTGAAACAGGACACAAGGCCTGTTACTAGCACT

CACATGGAACAAATGGCCCAGATCCTGGAGGCTTGCTGAAGGCTGTATGCTGACTCCAGGAATCTTACGG

ATTGTTTTGGCCACTGACTGACAATCCGTAATTCCTGGAGTCAGGACACAAGGCCTGTTACTAGCACTCA

CATGGAACAAATGGCCCAGATCCTGGAGGCTTGCTGAAGGCTGTATGCTGTCTGGCATCCGTTCAATGTT

GGTTTTGGCCACTGACTGACCAACATTGCGGATGCCAGACAGGACACAAGGCCTGTTACTAGCACTCACA

TGGAACAAATGGCCCAGATCTGGCCGCACTCGAGATATCTAGTGATCTAGAGGGCCCGCGGTTCGCTGAT

GGGGGAGGCTAACTGAAACACGGAAGGAGACAATACCGGAAGGAACCCGCGCTATGACGGCAATAAAAAG

ACAGAATAAAACGCACGGGTGTTGGGTCGTTTGTTCATAAACGCGGGGTTCGGTCCCAGGGCTGGCACTC

TGTCGATACCCCACCGTGACCCCATTGGGGCCAATACGCCCGCGTTTCTTCCTTTTCCCCACCCCACCCC

CCAAGTTCGGGTGAAGGCCCAGGGCTCGCAGCCAACGTCGGGGCGGCAGGCCCTGCCATAGCATCGATCG

CAAGCTT

Figure S13. Sequence of the tri-miR insert. Red, blue, green and violet letters indicate *Eco*RI, *Sal*I, *Bsu*15I and *Hin*dIII restriction sites, utilized in the cloning procedure; gray and black background indicate 5' and 3' miR flanking regions, respectively; red backgrounds correspond to 21-nt-long antisense target sequences (mature miRNA sequences), beginning in positions 475, 501 and 552 of hUTP24 ORF (from 5' to 3'); magenta backgrounds correspond to nucleotides 1-8 and 11-21 of the respective sense target sequences; green backgrounds represent a 19 nt-long sequence derived from endogenous murine miR-155, with underlined 13-nt-long segment able to form a loop within sh-miRNA structure; yellow background corresponds to HSV TK polyadenylation signal.

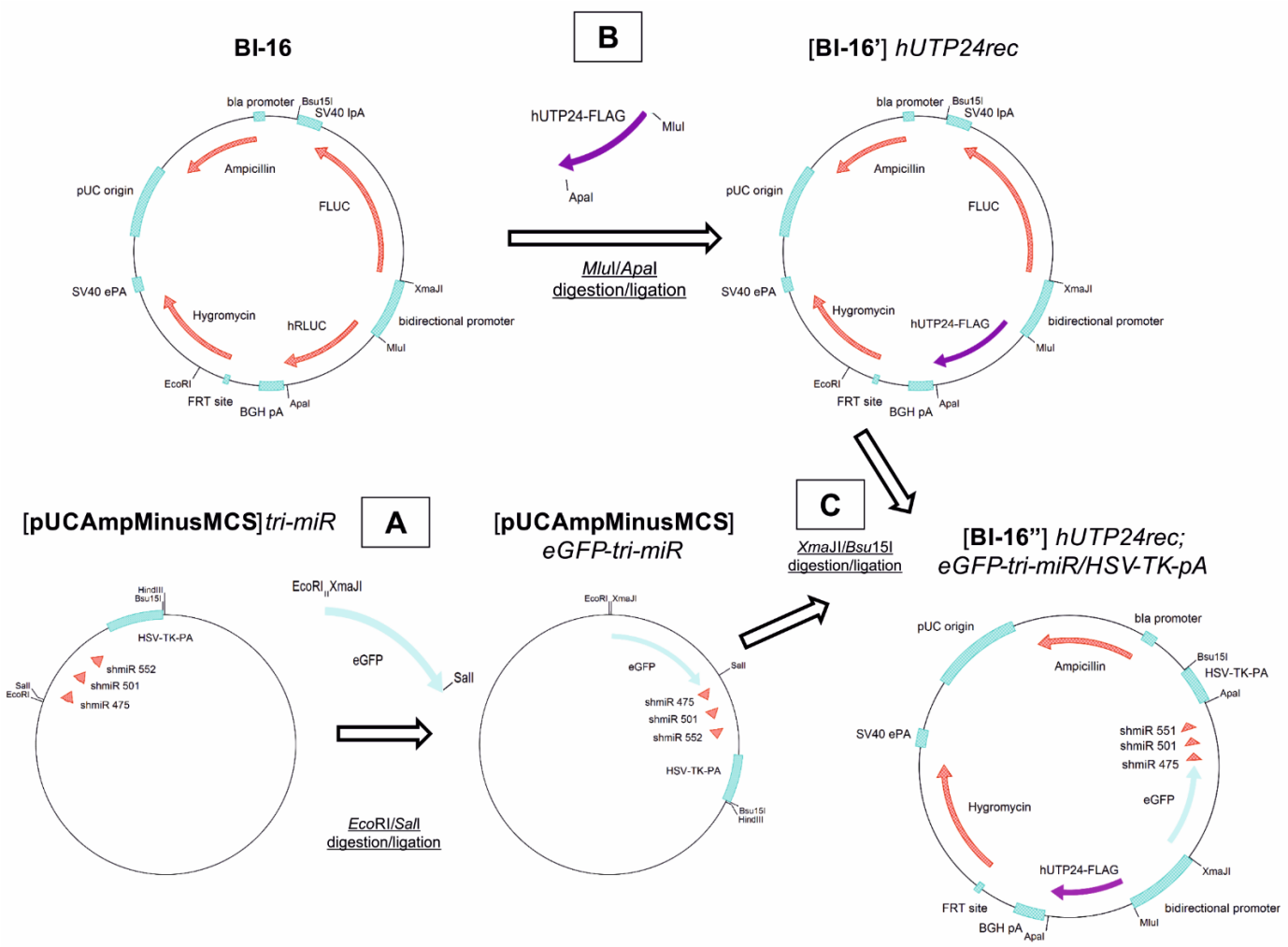

Figure S14. Outline of the cloning strategy, which was applied for the construction of vectors utilized for establishment of the model human cell lines producing WT and mut variants of hUTP24 protein. (**A**) First, a synthetic construct bearing three sh-miR sequences designed to specifically silence the expression of endogenous *hUTP24*, was ordered, and eGFP coding sequence was inserted into *Eco*RI and *Sal*I sites upstream sh-miRs, to enable monitoring of their expression. (**B**) In parallel, an insert encompassing recoded hUTP24 ORF (either wild-type or with catalytic mutation), which should be insensitive to sh-miRNA action, and FLAG epitope, was cloned into *Mlu*I/*Apa*I sites of the BI-16 vector. (**C**) Finally, a DNA fragment comprising fusion of eGFP with sh-miRs from step *A* was re-cloned into *Xma*JI/*Bsu*15I sites of BI-16 derivatives from step *B*, thus generating final constructs enabling simultaneous: 1) expression of a given variant of exogenous hUTP24-FLAG and 2) downregulation of endogenous *hUTP24*. Further details on the cloning procedure are described in the Supplemental Methods section.

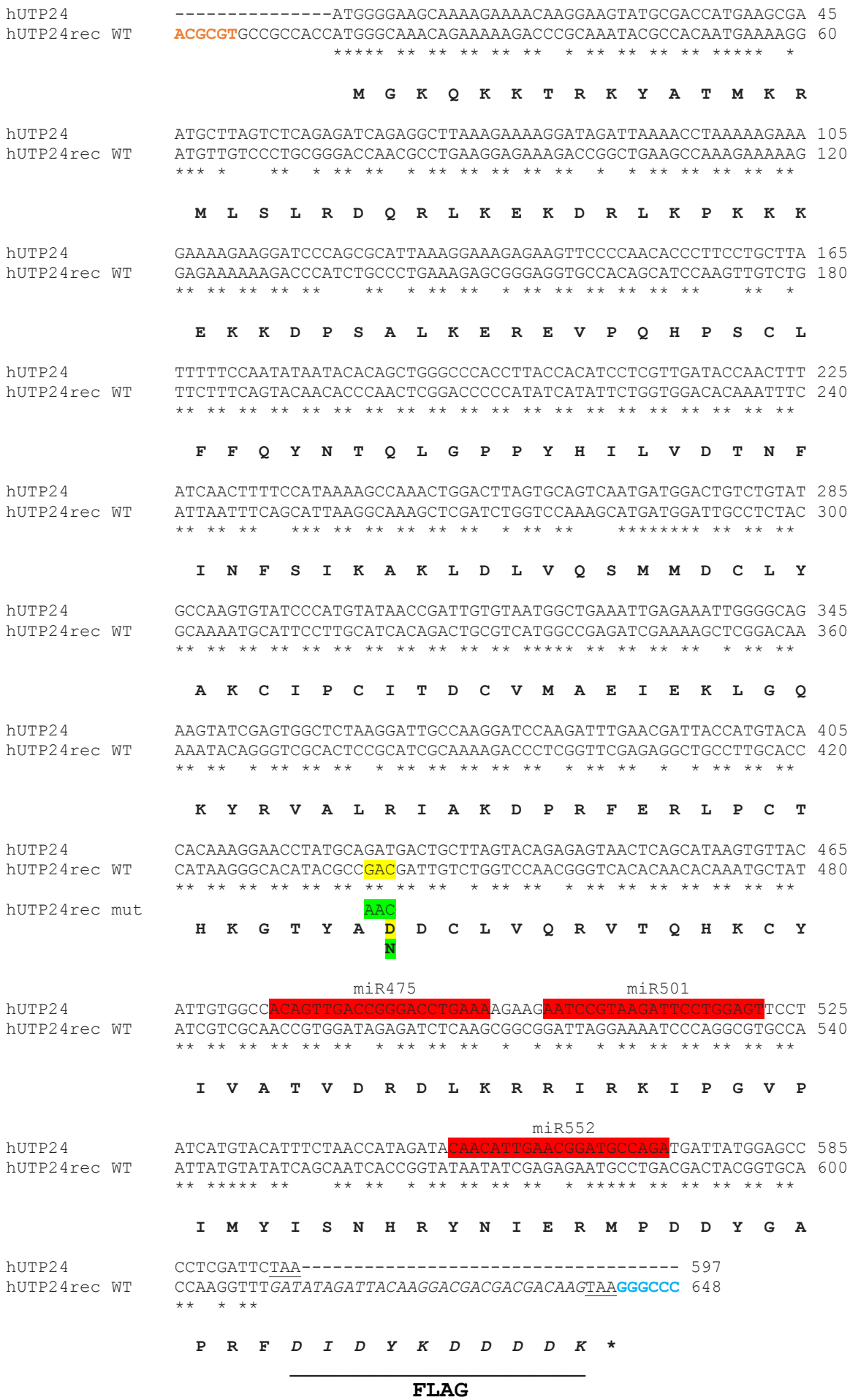
hUTP24 ----------ATGGGGAAGCAAAAGAAAACAAGGAAGTATGCGACCATGAAGCGA 45
hUTP24rec WT ACGCGTGCCGCCACCATGGGCAAACAGAAAAAGACCCGCAAATACGCCACAATGAAAAGG 60
M G K Q K K T R K Y A T M K R
hUTP24 ATGCTTAGTCTCAGAGATCAGAGGCTTAAAGAAAAGGATAGATTAAAACCTAAAAAGAAA 105
hUTP24rec WT ATGTTGTCCCTGCGGGACCAACGCCTGAAGGAGAAAGACCGGCTGAAGCCAAAGAAAAAG 120
M L S L R D Q R L K E K D R L K P K K K
hUTP24 GAAAAGAAGGATCCCAGCGCATTAAAGGAAAGAGAAGTTCCCCAACACCCTTCCTGCTTA 165
hUTP24rec WT GAGAAAAAAGACCCATCTGCCCTGAAAGAGCGGGAGGTGCCACAGCATCCAAGTTGTCTG 180
E K K D P S A L K E R E V P Q H P S C L
hUTP24 TTTTTCCAATATAATACACAGCTGGGCCCACCTTACCACATCCTCGTTGATACCAACTTT 225
hUTP24rec WT TTCTTTCAGTACAACACCCAACTCGGACCCCCATATCATATTCTGGTGGACACAAATTTC 240
F F Q Y N T Q L G P P Y H I L V D T N F
hUTP24 ATCAACTTTTCCATAAAAGCCAAACTGGACTTAGTGCAGTCAATGATGGACTGTCTGTAT 285
hUTP24rec WT ATTAATTTCAGCATTAAGGCAAAGCTCGATCTGGTCCAAAGCATGATGGATTGCCTCTAC 300
I N F S I K A K L D L V Q S M M D C L Y
hUTP24 GCCAAGTGTATCCCATGTATAACCGATTGTGTAATGGCTGAAATTGAGAAATTGGGGCAG 345
hUTP24rec WT GCAAAATGCATTCCTTGCATCACAGACTGCGTCATGGCCGAGATCGAAAAGCTCGGACAA 360
A K C I P C I T D C V M A E I E K L G Q
hUTP24 AAGTATCGAGTGGCTCTAAGGATTGCCAAGGATCCAAGATTTGAACGATTACCATGTACA 405
hUTP24rec WT AAATACAGGGTCGCACTCCGCATCGCAAAAGACCCTCGGTTCGAGAGGCTGCCTTGCACC 420
K Y R V A L R I A K D P R F E R L P C T
hUTP24 CACAAAGGAACCTATGCAGATGACTGCTTAGTACAGAGAGTAACTCAGCATAAGTGTTAC 465
hUTP24rec WT CATAAGGGCACATACGCCGACGATTGTCTGGTCCAACGGGTCACACAACACAAATGCTAT 480
hUTP24rec mut AAC
H K G T Y A D D C L V Q R V T Q H K C Y
N
miR475 miR501
hUTP24 ATTGTGGCCACAGTTGACCGGGACCTGAAAAGAAGAATCCGTAAGATTCCTGGAGTTCCT 525
hUTP24rec WT ATCGTCGCAACCGTGGATAGAGATCTCAAGCGGCGGATTAGGAAAATCCCAGGCGTGCCA 540
I V A T V D R D L K R R I R K I P G V P
miR552
hUTP24 ATCATGTACATTTCTAACCATAGATACAACATTGAACGGATGCCAGATGATTATGGAGCC 585
hUTP24rec WT ATTATGTATATCAGCAATCACCGGTATAATATCGAGAGAATGCCTGACGACTACGGTGCA 600
I M Y I S N H R Y N I E R M P D D Y G A
hUTP24 CCTCGATTCTAA---------- 597
hUTP24rec WT CCAAGGTTTGATATAGATTACAAGGACGACGACGACAAGTAAGGGCCC 648
P R F D I D Y K D D D D K *
FLAG

Figure S15. Alignment of the native (hUTP24) and recoded (hUTP24rec WT) wild-type hUTP24 ORF. Nucleotides unchanged during recoding are marked with asterisks; orange and blue letters indicate *Mlu*I and *Apa*I restriction sites, respectively; red backgrounds highlight positions of sequences targeted by pre-designed sh-miRs; green backgrounds indicate nucleotide (and resulting amino acid) difference in the hUTP24rec mutant variant; sequence coding for the FLAG epitope, present at the 3'-end of hUTP24rec insert is marked with italics; positions of translation termination codons are underlined.

Supplemental tables

Table S1. Bacterial and yeast strains used in this study

Strain	Genetic background	Source
MH1	*E. coli araD lacX74 galU hsdR hsdM rpsL*	[25]
dam-/dcm-	*E. coli ara-14 leuB6 fhuA31 lacY1 tsx78 glnV44 galK2 galT22 mcrA dcm-6 hisG4 rfbD1 R(zgb210::Tn10)* Tet^S *endA1 rspL136 (*Str^R*) dam13::Tn9 (*Cam^R*) xylA-5 mtl-1 thi-1 mcrB1 hsdR2*)	New England Biolabs; cat. no: C2925
BY4741	*S. cerevisiae MATa his3Δ1 leu2Δ0 met15Δ0 ura3Δ0*	[26]
yUTP24 tet::off	*S. cerevisiae pYDR339C::kanR-tet07-TATA URA3::CMV-tTA MATa his3Δ1 leu2Δ0 met15Δ0*	GE Healthcare; Yeast Tet-promoters Hughes (yTHC) Strain YDR339C; clone ID: TH_7562; cat. no: YSC1180-202219543
BMA64 diploid	*S. cerevisiae ade 2-1/ade 2-1 his3-11,15/his3-11,15 leu2-3,112/leu2-3,112 trp1Δ/trp1Δ ura3-1/ura3-1 can1-100/can1-100*	[27]
ADZY799	As BMA64, but with yUTP24 WT-TEV site-protein A tag-TRP selection marker cassette integrated into one allele of *UTP24* locus	this work
ADZY800	As BMA64, but with yUTP24 mut-TEV site-protein A tag-TRP selection marker cassette integrated into one allele of *UTP24* locus	this work

Table S2. Oligonucleotides used in this study

Oligonucleotide	Sequence (5'-3')	Purpose
ADZKD170	TGAGCGTAGGCGGTCACGCATACGTCATTGAAAAATTGCCAGATGTCT TTgagaatttgtattttcaggg	generation of ADZY799 strain
ADZKD171	ATAAACCAAAAACATTGCACTACATACTTAAAGAGTGAATACACAGTAG TTACGACTCACTATAGGG	generation of ADZY799 and ADZY800 strains
ADZKD172	CTCTTTAAACATTACTGTGC	validation of ADZY799 and ADZY800 strains
ADZKD173	GCTCACCCTGAAAATACAAATTCTC	validation of ADZY799 and ADZY800 strains
ADZKD174	AAAACAAGAAAGTTTGGCCTCG	generation of ADZY800 strain
ADZKD175	aaatacaaattctcAAAGACATCTGGCAATTTTTCAATGACG	generation of ADZY800 strain
ADZKD176	TTGCCAGATGTCTTTgagaatttgtattttcagg	generation of ADZY800 strain
yU24slicF	attgaagtctaccaggaacaaaccggt**ggatcc**ATGGGTAAAGCTAAGAAAAC	cloning of yUtp24 ORF into pET28M-6xHis-SUMOTag vector
yU24slicR	cggatctcagtggtggtggtggtggtg**ctcgag**TTAAAAGACATCTGGCAATT	cloning of yUtp24 ORF into pET28M-6xHis-SUMOTag vector
hU24slicF	attgaagtctaccaggaacaaaccggt**ggatcc**ATGGGGAAGCAAAAGAAAAC	cloning of hUTP24 ORF into pET28M-6xHis-SUMOTag vector
hU24slicR	cggatctcagtggtggtggtggtggtg**ctcgag**TTAGAATCGAGGGGCTCCAT	cloning of hUTP24 ORF into pET28M-6xHis-SUMOTag vector
yU24mutF	*CACAAGGG**tac**a**ta**CGCGAATGACTG*TTTAGTGCATCGAGTCTTAC	site-directed mutagenesis (yUtp24 D138N)
yU24mutR	*CAGTCATTCGCG**ta**t**gta**CCCTTGTG*CGAACAGCTTAGTCTCTTTATTC	site-directed mutagenesis (yUtp24 D138N)
hU24mutF	*CACAAAGG**tacgta**TGCAAATGACTG*CTTAGTACAGAGAGTAACTC	site-directed mutagenesis (hUTP24 D142N)
hU24mutR	*CAGTCATTTGCA**tacgta**CCTTTGTG*TGTACATGGTAATCGTTCAAATC	site-directed mutagenesis (hUTP24 D142N)
SumoF	TCATACTGTCAAAGACAGGG	sequencing of hDIS3 inserts in the [pET-28M-6xHis-SUMOTag] backbone
yU24cmpL	cgcg**tctaga**ATGGGTAAAGCTAAGAAAACAAG	cloning of yUtp24 ORF into p415 vector
yU24cmpR	aatt**gtcgac**TTAAAAGACATCTGGCAATTTTTCAATG	cloning of yUtp24 ORF into p415 vector
yU24flcmpR	aatt**gtcgac**TTA*cttatcgtcgtcatccttgtaatcCAT*AAAGACATCTGGCAATTT TTCAATG	cloning of yUtp24 ORF (+FLAG-tag) into p415 vector
hU24cmpL	cgcg**tctaga**ATGGGGAAGCAAAAGAAAACAAGG	cloning of hUTP24 ORF into p415 vector
hU24cmpR	aatt**gtcgac**TTAGAATCGAGGGGCTCCATAATCATCTGG	cloning of hUTP24 ORF into p415 vector

hU24flcmpR	aatt**gtcgac**TTA*cttatcgtcgtcatccttgtaatcCAT*GAATCGAGGGGCTCCATAATCATCTGG	cloning of hUTP24 ORF (+FLAG-tag) into p415 vector
p415-left	GTTTCCTCGTCATTGTTCTCG	sequencing of inserts in the [p415] backbone
0I.For	gga**GCTAGC**GAGAATTTGTATTTTCAGGGT**GATATC**CAGCACAGTGGCGG	construction of pcDNA5/FRT/TO(2xTEV)
0I.Rev	acc**ACCGGT**TCCTTGGAAGTA*CAG*GTTTTC**GGATCC**GAGCTC**GGTACC**AAG	construction of pcDNA5/FRT/TO(2xTEV)
0II.For	ggtcacctgtacaatcgatcctgcagga**GCTAGC**GAGAATTTGTATTTTC	construction of pcDNA5/FRT/TO(2xTEV)
0II.Rev	tcctgcaggatcgattgtacaggtgacc**ACCGGT**TCCTTGGAAGTA*CAG*G	construction of pcDNA5/FRT/TO(2xTEV)
p2.For	**gg**ACTCTAGCGTTTAAA**CTTAAG**CTTGGTACC***ATGGTGAGCAAGGGCGAGGAG***	construction of pcDNA5/FRT/TO(2xTEV)-N-eGFP
p2.Rev	cc**ACCGGT**TCCTTGGAAGTA*CAG*GTTTTC**GGATCC*TCTAGATCCGGTGGATCCCG***	construction of pcDNA5/FRT/TO(2xTEV)-N-eGFP
p3.For	**TATC**gattacaaggatgacgacgataag*TAG***CTCGAG**TCTAGAGGGCCCG	construction of pcDNA5/FRT/TO(2xTEV)-C-FLAG
p3.Rev	*CTA*cttatcgtcgtcatccttgtaatc**GATATC**ACCCTGAAAATACAAATTC	construction of pcDNA5/FRT/TO(2xTEV)-C-FLAG
p4.For	**CTAGC**GAGAATTTGTATTTTCAGGGT**GATATC*ATGGTGAGCAAGGGCGAGGAG***	construction of pcDNA5/FRT/TO(2xTEV)-C-eGFP
p4.Rev	GCGGGTTTAAACGGGCCCTCTAGA**CTCGAG*CTATCTAGATCCGGTGGATC***	construction of pcDNA5/FRT/TO(2xTEV)-C-eGFP
FRTT_F	TGACCTCCATAGAAGACACC	sequencing of inserts in the [pcDNA5/FRT/TO (2xTEV)] backbone
FRTT_R	AACTAGAAGGCACAGTCGAG	sequencing of inserts in the [pcDNA5/FRT/TO (2xTEV)] backbone
EGFP_F	CATGGTCCTGCTGGAGTTCG	sequencing of inserts in the [pcDNA5/FRT/TO (2xTEV)-N-eGFP] backbone
EGFP_R	TGAACTTGTGGCCGTTTACG	sequencing of inserts in the [pcDNA5/FRT/TO (2xTEV)-C-eGFP] backbone
hU24pcd5F	ggatccgaaaacctgtacttccaagga**accggt**ATGGGGAAGCAAAAGAAAAC	cloning of hUTP24 ORF into pcDNA5/FRT/TO-derived backbone
hU24pcd5R	gatatcaccctgaaaatacaaattctc**gctagc**GAATCGAGGGGCTCCATAATC	cloning of hUTP24 ORF into pcDNA5/FRT/TO-derived backbone (except pcDNA5/FRT/TO-N-eGFP)
hU24pcd5tR	gatatcaccctgaaaatacaaattctc**gctagc**TTAGAATCGAGGGGCTCCAT	cloning of hUTP24 ORF into pcDNA5/FRT/TO-N-eGFP

y18S oligo	CATGGCTTAATCTTTGAGAC (yeast rDNA: 753-734)	probe for northern blot; primer extension oligo
y25S oligo	CTCCGCTTATTGATATGC (yeast rDNA: 3309-3292)	probe for northern blot; primer extension oligo
y5ETS oligo	CGCTGCTCACCAATGG (yeast rDNA: 278-263)	probe for northern blot
yA0a oligo	ACTATCTTAAAAGAAGAAGCAACAAGCAG (yeast rDNA: 700-672)	probe for northern blot; primer extension oligo
yA0b oligo	CCAGATAACTATCTTAAAAG (yeast rDNA: 707-688)	primer extension oligo
yITS1a oligo	GAAACGGTTTTAATTGTCCTATAAC (yeast rDNA: 2704-2680)	probe for northern blot
yITS1b oligo	TGTTACCTCTGGGCCC (yeast rDNA: 2783-2768)	probe for northern blot; primer extension oligo
yITS2a oligo	GGCCAGCAATTTCAAGTTA (yeast rDNA: 3083-3065)	probe for northern blot; primer extension oligo
yITS2b oligo	AGATTAGCCGCAGTTGG (yeast rDNA: 3182-3166)	probe for northern blot; amplification of yeast rDNA fragment
y5.8S oligo	GCGTTCTTCATCGATGC (yeast rDNA: 2908-2892)	probe for northern blot
y5S oligo	CTACTCGGTCAGGCTC	probe for northern blot
h18S oligo	TTTACTTCCTCTAGATAGTCAAGTTCGACC (human rDNA: 5482-5453)	probe for northern blot
h5ETS oligo	CGGAGGCCCAACCTCTCCGACGACAGGTCGCCAGAGGACAGCGTGTCAGC (human rDNA: 50-1)	probe for northern blot
hITS1a oligo	CCTCGCCCTCCGGGCTCCGTTAATGATC (human rDNA: 5547-5520)	probe for northern blot
hITS1b oligo	AGGGGTCTTTAAACCTCCGCGCCGGAACGCGCTAGGTAC (human rDNA: 6159-6121)	probe for northern blot
hITS2a oligo	CTGCGAGGGAACCCCCAGCCGCGCA (human rDNA: 6845-6821)	probe for northern blot
hITS2b oligo	GCGCGACGGCGGACGACACCGCGGCGTC (human rDNA: 7591-7564)	probe for northern blot
h5.8S oligo	TCCTGCAATTCACATTAATTCTCGCAGCTAGC (human rDNA: 6702-6671)	probe for northern blot
h5S oligo	CATCCAAGTACTAACCAGGCCC	probe for northern blot
hA' oligo	GGTCCCGTTCGCCACGAACGTCCGCCCCTCG (human rDNA: 502-472)	probe for northern blot; primer extension oligo
hA0 oligo	TCACGCGCCGGACAGAG (human rDNA: 1747-1731)	probe for northern blot; primer extension oligo
hA1 oligo	GACATGCATGGCTTAATCTTTGAGACAAGC (human rDNA: 3714-3685)	primer extension oligo
h2 oligo	GGTTGCCTCAGGCCG (human rDNA: 6522-6508)	primer extension oligo
h5.8end	CTCGCAGCTAGCTGCGTTCTTCATCGAC (human rDNA: 6682-6655)	primer extension oligo
h5 oligo	CTTTTCCTCCGCTGACTAATATGCTTA (human rDNA: 7997-7971)	primer extension oligo
h28S oligo	CCCGTTCCCTTGGCTGTGGTTTCGCTGGATA (human rDNA: 11794-11764)	probe for northern blot
pEXseq1	ATGCGAAAGCAGTTGAAGAC (yeast rDNA: 1-20)	amplification of yeast rDNA fragment
pEXseq2	ATCGAAAGTTGATAGGGCAG (yeast rDNA: 1024-1005)	amplification of yeast rDNA fragment
pEXseq3	TCCGTAGGTGAACCTGCGG (yeast rDNA: 2471-2489)	amplification of yeast rDNA fragment
pEXseq4	TCGATGAAGAACGCAGCG (yeast rDNA: 2895-2912)	amplification of yeast rDNA fragment
pEXseq5	CCATCACTGTACTTGTTCGC (yeast rDNA: 3615-3596)	amplification of yeast rDNA fragment
3637For	TCGCCGCGCTCTACCTTACCTACC (human rDNA: 3637-3660)	amplification of human rDNA fragment
3971Rev	GATCGGCCCGAGGTTATCTAGAG (human rDNA: 3971-3949)	amplification of human rDNA fragment
eGFPFor	gcg**gaattc**atata**cctagg***ACC*ATGGTGAGCAAGGGCGAGGAGC	cloning of eGFP ORF into [pUCAmpMinusMCS] Backbone

eGFPRev	gcgc**gtcgac**TCACTACCTCCTC*TTA*CTTGTACAGCTCGTCCATGC	cloning of eGFP ORF into [pUCAmpMinusMCS] backbone
pUCmMCSF	GATTACGCCAAGCTCCTTCC	sequencing of eGFP ORF in [pUCAmpMinusMCS] backbone
pUCmMCSR	GCCAGTGAATTGGAGGCTAC	sequencing of eGFP ORF in [pUCAmpMinusMCS] backbone
BIseq_F	GATCGTCGGATCCTCTAGTC	sequencing of hUTP24 inserts in the [BI-16] vector backbone
BIseq_R	GCACAGTCGAGGCTGATCAG	sequencing of hUTP24 insert in the [BI-16] vector backbone
UTP_R330	TTTCGATCTCGGCCATGACG	sequencing of hUTP24 insert in the [BI-16] vector backbone
BI16seq1	CATTCTCCGCTCCATCGTTC	sequencing of eGFP-tri-miR insert in the [BI-16] vector backbone
BI16seq2	TCCACTGGTCGACTCACTAC	sequencing of eGFP-tri-miR inserts in the [BI-16] vector backbone
miR-U475 oligo	ACAGTTGACCGGGACCTGAAA	probe for northern blot
miR-U501 oligo	AATCCGTAAGATTCCTGGAGT	probe for northern blot
miR-U552 oligo	CAACATTGAACGGATGCCAGA	probe for northern blot
GAPDH_RT (for/rev)	GTCAGCCGCATCTTCTTTTG / GCGCCCAATACGACCAAATC	qPCR primer pair
hUTP24_RT1 (for/rev)	GGATCCCAGCGCATTAAAGG / ACGAGGATGTGGTAAGGTGG	qPCR primer pair
hUTP24_RT2 (for/rev)	GCCCACCTTACCACATCCTC / ACTTGGCATACAGACAGTCCA	qPCR primer pair
CamKI mRNA_RT (for/rev)	AGGCGGAGGACATTAGAGAC / TTGATCTTGTGCAGGACAGC	qPCR primer pair
CamKI In1J_RT (for/rev)	TGCAGGTTGAATGACTGAATGG / TCTCGGAAGTCGTAGATGTCTC	qPCR primer pair
CamKI In2J_RT (for/rev)	AGGCGGAGGACATTAGAGAC / AAGTGAAAAGCTGGGGACAG	qPCR primer pair

Table S3. Plasmids used in this study

Plasmid	Source or genotype
pET28M-6xHis-SUMOTag	[28, 29]
pU24-1	[pET28M-6xHis-SUMOTag] *yUtp24 WT*
pU24-2	[pET28M-6xHis-SUMOTag] *hUTP24 WT*
pU24-3	[pET28M-6xHis-SUMOTag] *yUtp24 mut (D138N)*
pU24-4	[pET28M-6xHis-SUMOTag] *hUTP24 mut (D142N)*
p415	[30, 31]
pU24-5	[p415] *yUtp24 WT*
pU24-6	[p415] *yUtp24 WT-FLAG*
pU24-7	[p415] *yUtp24 mut*
pU24-8	[p415] *yUtp24 mut-FLAG*
pU24-9	[p415] *hUTP24 WT*
pU24-10	[p415] *hUTP24 WT-FLAG*
pU24-11	[p415] *hUTP24 mut*
pU24-12	[p415] *hUTP24 mut-FLAG*
pBS1479	[32]
pCR™-Blunt II-Topo®	Invitrogen
pU24-13	[Topo] yeast rDNA 1-1024
pU24-14	[Topo] yeast rDNA 2471-3182
pU24-15	[Topo] yeast rDNA 2895-3615
pU24-16	[Topo] human rDNA 3637-3615
pcDNA5/FRT/TO	Invitrogen
pcDNA5/FRT/TO(2xTEV)	this work
pcDNA5/FRT/TO(2xTEV)-C-FLAG	this work
pEGFP-C1	Clontech
pcDNA5/FRT/TO	Invitrogen
pcDNA5/FRT/TO(2xTEV)-N-eGFP	this work
pcDNA5/FRT/TO(2xTEV)-C-eGFP	this work
pU24-17	[pcDNA5/FRT/TO(2xTEV)-FLAG] *hUTP24 WT*
pU24-18	[pcDNA5/FRT/TO(2xTEV)-FLAG] *hUTP24 mut*
pU24-19	[pcDNA5/FRT/TO(2xTEV)-N-eGFP] *hUTP24 WT*
pU24-20	[pcDNA5/FRT/TO(2xTEV)-C-eGFP] *hUTP24 WT*
pU24-21	[pcDNA5/FRT/TO(2xTEV)-C-eGFP] *hUTP24 mut*
BI-16	[33]
pEGFP-N1	Clontech
pU24-22	[BI-16''] *hUTP24rec WT; eGFP-tri-miR/HSV-TK-PA*
pU24-23	[BI-16''] *hUTP24rec mut; eGFP-tri-miR/HSV-TK-PA*

Supplemental References

1. Samarsky DA, Fournier MJ. Functional mapping of the U3 small nucleolar RNA from the yeast *Saccharomyces cerevisiae*. Mol Cell Biol 1998; 18:3431-44; PMID:9584183
2. Mereau A, Fournier R, Gregoire A, Mougin A, Fabrizio P, Luhrmann R, Branlant C. An *in vivo* and *in vitro* structure-function analysis of the *Saccharomyces cerevisiae* U3A snoRNP: protein-RNA contacts and base-pair interaction with the pre-ribosomal RNA. J Mol Biol 1997; 273:552-71; PMID:9356246; http://dx.doi.org/10.1006/jmbi.1997.1320
3. Hughes JM. Functional base-pairing interaction between highly conserved elements of U3 small nucleolar RNA and the small ribosomal subunit RNA. Journal of molecular biology 1996; 259:645-54; PMID:8683571; http://dx.doi.org/10.1006/jmbi.1996.0346
4. Sharma K, Tollervey D. Base pairing between U3 small nucleolar RNA and the 5' end of 18S rRNA is required for pre-rRNA processing. Mol Cell Biol 1999; 19:6012-9; PMID:10454548
5. Borovjagin AV, Gerbi SA. *Xenopus* U3 snoRNA GAC-Box A' and Box A sequences play distinct functional roles in rRNA processing. Mol Cell Biol 2001; 21:6210-21; PMID:1150966; http://dx.doi.org/10.1128/MCB.21.18.6210-6221.2001
6. Beltrame M, Tollervey D. Identification and functional analysis of two U3 binding sites on yeast pre-ribosomal RNA. EMBO J 1992; 11:1531-42; PMID:1563354
7. Beltrame M, Henry Y, Tollervey D. Mutational analysis of an essential binding site for the U3 snoRNA in the 5' external transcribed spacer of yeast pre-rRNA. Nucleic Acids Res 1994; 22:4057-65; PMID:7800512; http://dx.doi.org/10.1093/nar/22.23.5139
8. Beltrame M, Tollervey D. Base pairing between U3 and the pre-ribosomal RNA is required for 18S rRNA synthesis. EMBO J 1995; 14:4350-6; PMID:7556076
9. Dutca LM, Gallagher JE, Baserga SJ. The initial U3 snoRNA:pre-rRNA base pairing interaction required for pre-18S rRNA folding revealed by in vivo chemical probing. Nucleic Acids Res 2011; 39:5164-80; PMID:21349877; http://dx.doi.org/10.1093/nar/gkr044
10. Marmier-Gourrier N, Clery A, Schlotter F, Senty-Segault V, Branlant C. A second base pair interaction between U3 small nucleolar RNA and the 5'-ETS region is required for early cleavage of the yeast pre-ribosomal RNA. Nucleic Acids Res 2011; 39:9731-45; PMID:21890904; http://dx.doi.org/10.1093/nar/gkr675
11. Borovjagin AV, Gerbi SA. The spacing between functional Cis-elements of U3 snoRNA is critical for rRNA processing. Journal Mol Biol 2000; 300:57-74; PMID:10864498; http://dx.doi.org/10.1006/jmbi.2000.3798
12. Borovjagin AV, Gerbi SA. *Xenopus* U3 snoRNA docks on pre-rRNA through a novel base-pairing interaction. RNA 2004; 10:942-53; PMID:15146078; http://dx.doi.org/10.1261/rna.5256704
13. Borovjagin AV, Gerbi SA. An evolutionary intra-molecular shift in the preferred U3 snoRNA binding site on pre-ribosomal RNA. Nucleic Acids Res 2005; 33:4995-5005; PMID:16147982; http://dx.doi.org/10.1093/nar/gki815
14. Hartshorne T. Distinct regions of U3 snoRNA interact at two sites within the 5' external transcribed spacer of pre-rRNAs in *Trypanosoma brucei* cells. Nucleic Acids Res 1998; 26:2541-53; PMID:9592135; http://dx.doi.org/10.1093/nar/26.11.2541
15. Kass S, Tyc K, Steitz JA, Sollner-Webb B. The U3 small nucleolar ribonucleoprotein functions in the first step of preribosomal RNA processing. Cell 1990; 60:897-908; PMID:2156625; http://dx.doi.org/10.1016/0092-8674(90)90338-F
16. Craig N, Kass S, Sollner-Webb B. Sequence organization and RNA structural motifs directing the mouse primary rRNA-processing event. Mol Cell Biol 1991; 11:458-67; PMID:1986240; http://dx.doi.org/10.1128/MCB.11.1.458
17. Kass S, Craig N, Sollner-Webb B. Primary processing of mammalian rRNA involves two adjacent cleavages and is not species specific. Molecular and cellular biology 1987; 7:2891-8; PMID:3670298; http://dx.doi.org/10.1128/MCB.7.8.2891
18. Hartshorne T, Toyofuku W. Two 5'-ETS regions implicated in interactions with U3 snoRNA are required for small subunit rRNA maturation in *Trypanosoma brucei*. Nucleic Acids Res 1999; 27:3300-9; PMID:10454637; http://dx.doi.org/10.1093/nar/27.16.3300

19. Savino R, Gerbi SA. Preribosomal RNA processing in *Xenopus* oocytes does not include cleavage within the external transcribed spacer as an early step. Biochimie 1991; 73:805-12; PMID:1764525; http://dx.doi.org/10.1016/0300-9084(91)90060-E
20. Hartshorne T, Toyofuku W, Hollenbaugh J. *Trypanosoma brucei* 5'ETS A'-cleavage is directed by 3'-adjacent sequences, but not two U3 snoRNA-binding elements, which are all required for subsequent pre-small subunit rRNA processing events. J Mol Biol 2001; 313:733-49; PMID:11697900; http://dx.doi.org/10.1006/jmbi.2001.5078
21. Ginisty H, Amalric F, Bouvet P. Nucleolin functions in the first step of ribosomal RNA processing. The EMBO J 1998; 17:1476-86; PMID:9482744; http://dx.doi.org/10.1093/emboj/17.5.1476
22. Ginisty H, Serin G, Ghisolfi-Nieto L, Roger B, Libante V, Amalric F, Bouvet P. Interaction of nucleolin with an evolutionarily conserved pre-ribosomal RNA sequence is required for the assembly of the primary processing complex. J Biol Chem 2000; 275:18845-50; PMID:10858445; http://dx.doi.org/10.1074/jbc.M002350200
23. Pertschy B, Schneider C, Gnadig M, Schafer T, Tollervey D, Hurt E. RNA helicase Prp43 and its co-factor Pfa1 promote 20 to 18 S rRNA processing catalyzed by the endonuclease Nob1. J Biol Chem 2009; 284:35079-91; PMID:19801658; http://dx.doi.org/10.1074/jbc.M109.040774
24. Borovjagin AV, Gerbi SA. *Xenopus* U3 snoRNA GAC-Box A' and Box A sequences play distinct functional roles in rRNA processing. Mol Cell Biol 2001; 21:6210-21; PMID:1150966; http://dx.doi.org/10.1128/MCB.21.18.6210-6221.2001
25. Goddard JM, Caput D, Williams SR, Martin DW, Jr. Cloning of human purine-nucleoside phosphorylase cDNA sequences by complementation in *Escherichia coli*. Proc Natl Acad Sci USA 1983; 80:4281-5; PMID:6410388
26. Brachmann CB, Davies A, Cost GJ, Caputo E, Li J, Hieter P, Boeke JD. Designer deletion strains derived from *Saccharomyces cerevisiae* S288C: a useful set of strains and plasmids for PCR-mediated gene disruption and other applications. Yeast 1998; 14:115-32; PMID:9483801; http://dx.doi.org/10.1002/(SICI)1097-0061(19980130)14:2<115::AID-YEA204>3.0.CO;2-2
27. Baudin-Baillieu A, Guillemet E, Cullin C, Lacroute F. Construction of a yeast strain deleted for the TRP1 promoter and coding region that enhances the efficiency of the polymerase chain reaction-disruption method. Yeast 1997; 13:353-6; PMID:9133738; http://dx.doi.org/10.1002/(SICI)1097-0061(19970330)13:4<353::AID-YEA86>3.0.CO;2-P
28. Lebreton A, Tomecki R, Dziembowski A, Seraphin B. Endonucleolytic RNA cleavage by a eukaryotic exosome. Nature 2008; 456:993-6; PMID:19060886; http://dx.doi.org/10.1038/nature07480
29. Malakhov MP, Mattern MR, Malakhova OA, Drinker M, Weeks SD, Butt TR. SUMO fusions and SUMO-specific protease for efficient expression and purification of proteins. J Struct Funct Genomics 2004; 5:75-86; PMID:15263846; http://dx.doi.org/10.1002/(SICI)1097-0061(19970330)13:4<353::AID-YEA86>3.0.CO;2-P
30. Mumberg D, Muller R, Funk M. Yeast vectors for the controlled expression of heterologous proteins in different genetic backgrounds. Gene 1995; 156:119-22; PMID:7737504; http://dx.doi.org/10.1016/0378-1119(95)00037-7
31. Mumberg D, Muller R, Funk M. Regulatable promoters of *Saccharomyces cerevisiae*: comparison of transcriptional activity and their use for heterologous expression. Nucleic Acids Res 1994; 22:5767-8; PMID:7838736; http://dx.doi.org/10.1093/nar/22.25.5767
32. Puig O, Caspary F, Rigaut G, Rutz B, Bouveret E, Bragado-Nilsson E, Wilm M, Seraphin B. The tandem affinity purification (TAP) method: a general procedure of protein complex purification. Methods 2001; 24:218-29; PMID:11403571; http://dx.doi.org/10.1006/meth.2001.1183
33. Sammarco MC, Grabczyk E. A series of bidirectional tetracycline-inducible promoters provides coordinated protein expression. Anal Biochem 2005; 346:210-6; PMID:16212928; http://dx.doi.org/10.1016/j.ab.2005.08.033